Trefftz Finite Element Method and Its Applications

Qing-Hua Qin
Department of Engineering,
Australian National University,
Canberra ACT 0200, Australia

This paper presents an overview of the Trefftz finite element and its application in various engineering problems. Basic concepts of the Trefftz method are discussed, such as T-complete functions, special purpose elements, modified variational functionals, rank conditions, intraelement fields, and frame fields. The hybrid-Trefftz finite element formulation and numerical solutions of potential flow problems, plane elasticity, linear thin and thick plate bending, transient heat conduction, and geometrically nonlinear plate bending are described. Formulations for all cases are derived by means of a modified variational functional and T-complete solutions. In the case of geometrically nonlinear plate bending, exact solutions of the Lamé-Navier equations are used for the in-plane intraelement displacement field, and an incremental form of the basic equations is adopted. Generation of elemental stiffness equations from the modified variational principle is also discussed. Some typical numerical results are presented to show the application of the finite element approach. Finally, a brief summary of the approach is provided and future trends in this field are identified. There are 151 references cited in this revised article.
[DOI: 10.1115/1.1995716]

1 Introduction

During past decades the hybrid-Trefftz (HT) finite element (FE) model, originating about 27 years ago [1,2], has been considerably improved and has now become a highly efficient computational tool for the solution of complex boundary value problems. In contrast to conventional FE models, the class of finite elements associated with the Trefftz method is based on a hybrid method that includes the use of an auxiliary interelement displacement or traction frame to link the internal displacement fields of the elements. Such internal fields, chosen so as to a priori satisfy the governing differential equations, have conveniently been represented as the sum of a particular integral of nonhomogeneous equations and a suitably truncated T-complete set of regular homogeneous solutions multiplied by undetermined coefficients. The mathematical fundamentals of the T-complete set have been laid out mainly by Herrera and co-workers [3–6] who named this system a C-complete system. Following a suggestion by Zienkiewicz, he changed this to the T-complete (Trefftz-complete) system of solutions, in honor of the originator of such nonsingular solutions. As such, the terminology "TH-families" is usually used when referring to systems of functions that satisfy the criterion originated by Herrera [4]. Interelement continuity is enforced by using a modified variational principle together with an independent frame field defined on each element boundary. The element formulation, during which the internal parameters are eliminated at the element level, leads to the standard force-displacement relationship, with a symmetric positive definite stiffness matrix. Clearly, although the conventional FE formulation may be assimilated to a particular form of the Rayleigh-Ritz method, the HT FE approach has a close relationship with the Trefftz method [7]. As noted in [8,9], the main advantages stemming from the HT FE model are (i) the formulation calls for integration along the element boundaries only, which enables arbitrary polygonal or even curve-sided elements to be generated. As a result, it may be considered as a special, symmetric, substructure-oriented boundary solution approach and, thus, possesses the advantages of the boundary element method (BEM). In contrast to conventional boundary element formulation, however, the HT FE model avoids the introduction of singular integral equations and does not require the construction of a fundamental solution, which may be very laborious to build; (ii) the HT FE model is likely to represent the optimal expansion bases for hybrid-type elements where interelement continuity need not be satisfied, a priori, which is particularly important for generating a quasi-conforming plate-bending element; (iii) the model offers the attractive possibility of developing accurate crack-tip, singular corner, or perforated elements, simply by using appropriate known local solution functions as the trial functions of intraelement displacements.

The first attempt to generate a general purpose HT FE formulation occurred in the study by Jirousek and Leon [2] of the effect of mesh distortion on thin-plate elements. It was immediately noted that T-complete functions represented an optimal expansion basis for hybrid-type elements where interelement continuity need not be satisfied a priori. Since then, the Trefftz-element concept has become increasingly popular, attracting a growing number of researchers into this field [10–23]. Trefftz-elements have been successfully applied to problems of elasticity [24–28], Kirchhoff plates [8,22,29–31], moderately thick Reissner-Mindlin plates [32–36], thick plates [37–39], general three-dimensional (3D) solid mechanics [20,40], axisymmetric solid mechanics [41], potential problems [42,43], shells [44], elastodynamic problems [16,45–47], transient heat conduction analysis [48], geometrically nonlinear plates [49–52], materially nonlinear elasticity [53–55], and piezoelectric materials [56,57]. Furthermore, the concept of special purpose functions has been found to be of great efficiency in dealing with various geometry or load-dependent singularities and local effects (e.g., obtuse or reentrant corners, cracks, circular or elliptic holes, concentrated or patch loads, see [24,25,27,30,58] for details). In addition, the idea of developing p versions of Trefftz elements, similar to those used in the conventional FE model, was presented in 1982 [24] and has already been shown to be particularly advantageous from the point of view of both computation and facilities for use [13,59]. Huang and Li [60] presented an Adini's element coupled with the Trefftz method, which is suitable for modeling singular problems. The first monograph to describe, in detail, the HT FE approach and its applications in solid mechanics was published recently [61]. Moreover, a wealthy source of information pertaining to the HT FE approach exists in a number of general or special review type of articles, such as those of Herrera [12,62], Jirousek [63], Jirousek and Wroblewski [9,64], Jirousek and Zielinski [65], Kita and Kamiya [66], Qin [67,68], and Zienkiewicz [69].

Another related approach, called the indirect Trefftz approach,

Transmitted by Associate Editor S. Adali.

deals with any linear system regardless of whether it is symmetric or nonsymmetric [62]. The method is based on local solutions of the adjoint differential equations and provides information about the sought solution at internal boundaries. Many developments and applications of the method have been made during the past decades. For example, some theoretical results for symmetric systems can be found in [3,4,6,70,71]. Numerical applications were reported in [72,73]. Based on this approach a localized adjoint method was precented in [5,74]. More Recently, Herrera and his coworkers developed the advanced theory of domain decomposition methods [75–79] and produced corresponding numerical results [80,81].

Variational functionals are essential and play a central role in the formulation of the fundamental governing equations in the Trefftz FE method. They are the heart of many numerical methods, such as boundary element methods, finite volume methods, and Trefftz FE methods [61]. During past decades, much work has been done concerning variational formulations for Trefftz numerical methods [27,61,82–85]. Herrera [82] presented a variational formulation that is for problems with or without discontinuities using Trefftz method. Piltner [27] presented two different variational formulations to treat special elements with holes or cracks. The formulations consist of a conventional potential energy and a least-squares functional. The least-squares functional was not added as a penalty function to the potential functional, but is minimized separately for the special elements considered. Jirousek [84] developed a variational functional in which either the displacement conformity or the reciprocity of the conjugate tractions is enforced at the element interfaces. Jirousek and Zielinski [85] obtained two complementary hybrid Trefftz formulations based on the weighted residual method. The dual formulations enforced the reciprocity of boundary traction more strongly than the conformity of the displacement fields. Qin [61] presented a modified variational principle based hybrid-Trefftz displacement frame.

Applying T-complete solution functions, Zielinski and Zienkiewicz [43] presented a solution technique in which the boundary solutions over subdomains are linked by least-squares procedures without an auxiliary frame. Cheung et al. [86,87] developed a set of indirect and direct formulations using T-complete systems of Trefftz functions for Poisson and Helmholtz equations. Jirousek and Stojek [42] and Jirousek and Wroblewski [88] studied an alternative method, called "frameless" T-element approach, based on the application of a suitably truncated T-complete set of Trefftz functions, over individual subdomains linked by means of a least-squares procedure, and applied it to Poisson's equation. Stojek [89] extended their work to the case of the Helmholtz equation. In addition, the work should be mentioned here of Cialkowski [90], Desmet et al. [91], Hsiao et al. [92], Ihlenburg and Babuska [93], Kita et al. [94], Kolodziej and Mendes [95], Kolodziej and Uscilowska [96], Stojek et al. [97], and Zielinski [98], in connection with potential flow problems.

The first application of the HT FE approach to plane elastic problems appears to be that of Jirousek and Teodorescu [24]. That paper deals with two alternative variational formulations of HT plane elasticity elements, depending on whether the auxiliary frame function displacement field is assumed along the whole element boundary or confined only to the interelement portion. Subsequently, various versions of HT elasticity elements have been presented by Freitas and Bussamra [99], Freitas and Cismasiu [100], Hsiao et al. [101], Jin et al. [102], Qin [103], Jirousek and Venkatesh [25], Kompis et al. [104,105], Piltner [27,40], Sladek and Sladek [106], and Sladek et al. [107]. Most of the developments in this field are described in a recent review paper by Jirousek and Wroblewski [9].

Extensions of the Trefftz method to plate bending have been the subject of fruitful scientific preoccupation of many a distinguished researcher (e.g., [22,29,31,58,108,109]). Jirousek and Leon [2] pioneered the application of T-elements to plate bending problems. Since then, various plate elements based on the hybrid-Trefftz approach have been presented, such as h and p elements [29], nine-degree-of-freedom (DOF) triangular elements [30] and an improved version [110], and a family of 12-DOF quadrilateral elements [33]. Extensions of this procedure have been reported for thin plate on an elastic foundation [22], for transient plate-bending analysis [47], and for postbuckling analysis of thin plates [49]. Alternatively, Jin et al. [108] developed a set of formulations, called Trefftz direct and indirect methods, for plate-bending problems based on the weighted residual method.

Based on the Trefftz method, a hierarchic family of triangular and quadrilateral T-elements for analyzing moderately thick Reissner-Mindlin plates was presented by Jirousek et al. [33,34] and Petrolito [37,38]. In these HT formulations, the displacement and rotation components of the auxiliary frame field $\tilde{\mathbf{u}} = \{\tilde{w}, \tilde{\psi}_x, \tilde{\psi}_y\}^T$, used to enforce conformity on the internal Trefftz field $\mathbf{u} = \{w, \psi_x, \psi_y\}^T$, are independently interpolated along the element boundary in terms of nodal values. Jirousek et al. [33] showed that the performance of the HT thick plate elements could be considerably improved by the application of a linked interpolation whereby the boundary interpolation of the displacement $\tilde{w}$ is linked through a suitable constraint with that of the tangential rotation component.

Applications of the Trefftz FE method to other fields can be found in the work of Brink et al. [111], Chang et al. [112], Freitas [113], Gyimesi et al. [114], He [115], Herrera et al. [79], Jirousek and Venkatesh [116], Karaś and Zieliński [117], Kompis and Jakubovicova [118], Olegovich [119], Onuki et al. [120], Qin [56,57], Reutskiy [121], Szybiński et al. [122], Wroblewski et al. [41], Zieliński and Herrera [123], and Zieliński et al. [124].

Following this introduction, the present review consists of 11 sections. Basic concepts and general element formulations of the method, which include basic descriptions of a physical problem, two groups of independently assumed displacement fields, Trefftz functions, and modified variational functions, are described in Sec. 2. Section 3 focuses on the essentials of Trefftz elements for linear potential problems based on Trefftz functions and the modified variational principle appearing in Sec. 2. It describes, in detail, the method of deriving Trefftz functions, element stiffness equations, the concept of rank condition, and special-purpose functions accounting for local effects. The applications of Trefftz elements to linear elastic problems, thin-plate bending, thick plate, and transient heat conduction are described in Sec. 4–7. Extensions of the process to geometrically nonlinear problems of plates is considered in Sec. 8 and 9. A variety of numerical examples are presented in Sec. 10 to illustrate the applications of the Trefftz FE method. Finally, a brief summary of the developments of the Treffz FE approach is provided, and areas that need further research are identified.

2 Basic Formulations for Trefftz FE Approach

In this section, some important preliminary concepts, emphasizing Trefftz functions, modified variational principles, and elemental stiffness matrix, are reviewed. The following descriptions are based on the work of Jirousek and Wroblewski [9], Jirousek and Zielinski [65], and Qin [61]. In the following, a right-hand Cartesian coordinate system is adopted, the position of a point is denoted by $\mathbf{x}$ (or x_i), and both conventional indicial notation (x_i) and traditional Cartesian notation (x, y, z) are utilized. In the case of indicial notation we invoke the summation convention over repeated indices. Vectors, tensors, and their matrix representations are denoted by boldface letters.

2.1 Basic Relationships in Engineering Problems. Most of the physical problems in various branches of engineering are boundary value problems. Any numerical solution to these problems must satisfy the basic equations of equilibrium, boundary conditions, and so on. For a practical problem, physical behavior is governed by the following field equations:

$$\mathbf{L}\boldsymbol{\sigma}+\bar{\mathbf{b}}=0 \quad \text{(partial differential equation)} \tag{1}$$

$$\boldsymbol{\sigma}=\mathbf{D}\boldsymbol{\varepsilon} \quad \text{(constitutive law)} \tag{2}$$

$$\boldsymbol{\varepsilon}=\mathbf{L}^T\mathbf{u} \quad \text{(generalized geometrical relationship)} \tag{3}$$

with the boundary conditions

$$\mathbf{u}=\bar{\mathbf{u}} \quad (\text{on } \Gamma_u, \text{ essential boundary condition}) \tag{4}$$

$$\mathbf{t}=\mathbf{A}\boldsymbol{\sigma}=\bar{\mathbf{t}} \quad (\text{on } \Gamma_t, \text{ natural boundary condition}) \tag{5}$$

where the matrix notation $\mathbf{u}$, $\boldsymbol{\varepsilon}$, $\boldsymbol{\sigma}$, and $\bar{\mathbf{b}}$ are vectors of generalized displacements, strains, stresses, and body forces; $\mathbf{L}$, $\mathbf{D}$, and $\mathbf{A}$ stand for differential operator matrix, constitutive coefficient matrix, and transformation matrix, respectively, including the components of the external normal unit vector of the boundary. In the Trefftz FE form, Eqs. (1)–(5) should be completed by adding the following interelement continuity requirements:

$$\mathbf{u}_e=\mathbf{u}_f \quad (\text{on } \Gamma_e \cap \Gamma_f, \text{ conformity}) \tag{6}$$

$$\mathbf{t}_e+\mathbf{t}_f=0 \quad (\text{on } \Gamma_e \cap \Gamma_f, \text{ traction reciprocity}) \tag{7}$$

where e and f stand for any two neighboring elements. With suitably defined matrices $\mathbf{L}$, $\mathbf{D}$, and $\mathbf{A}$, one can describe a particular physical problem through the general relationships (1)–(7). The first step in a FE analysis is, therefore, to decide what kind of problem is at hand. This decision is based on the assumptions used in the theory of physical and mathematical approaches to the solution of specific problems. Some typical problems encountered may involve: (i) beam, (ii) heat conduction, (iii) electrostatics, (iv) plane stress, (v) plane strain, (vi) plate bending, (viii) moderately thick plate, and (ix) general three-dimensional elasticity. As an illustration, let us consider plane stress problem. For this special problem, we have

$$\mathbf{u}=\{u\ v\}^T, \quad \bar{\mathbf{b}}=\{\bar{b}_x\ \bar{b}_y\}^T, \quad \boldsymbol{\varepsilon}=\{\varepsilon_{xx}\ \varepsilon_{yy}\ 2\varepsilon_{xy}\}^T,$$
$$\boldsymbol{\sigma}=\{\boldsymbol{\sigma}_{xx}\ \boldsymbol{\sigma}_{yy}\ \boldsymbol{\sigma}_{xy}\}^T$$
$$\mathbf{v}=\{u\ v\}^T, \quad \mathbf{L}=\begin{bmatrix} \partial/\partial x & 0 & \partial/\partial y \\ 0 & \partial/\partial y & \partial/\partial x \end{bmatrix}$$
$$\mathbf{D}=\frac{E}{1-\mu^2}\begin{bmatrix} 1 & \mu & 0 \\ \mu & 1 & 0 \\ 0 & 0 & \dfrac{1-\mu}{2} \end{bmatrix}, \quad \mathbf{A}=\begin{bmatrix} n_x & 0 & n_y \\ 0 & n_y & n_x \end{bmatrix},$$
$$\mathbf{t}=\mathbf{A}\boldsymbol{\sigma}=\{t_1,t_2\}^T \tag{8}$$

where u, v, and $\bar{b}_i$ are, respectively, displacements in the x and y directions and body forces; $\boldsymbol{\varepsilon}_{ij}$ and $\boldsymbol{\sigma}_{ij}$ are strains and stresses, respectively; E and μ are Young's modulus and Poisson's ratio; n_i are components of the external normal unit vector; and t_i are components of surface traction.

2.2 Assumed Fields. The main idea of the HT FE model is to establish a finite element formulation whereby interelement continuity is enforced on a nonconforming internal field chosen so as to a priori satisfy the governing differential equation of the problem under consideration [61]. In other words, as an obvious alternative to the Rayleigh-Ritz method as a basis for a FE formulation, the model here is based on the method of Trefftz [7], for which Herrera [75] gave a general definition as: *Given a region of an Euclidean space of some partitions of that region, a "Trefftz Method" is any procedure for solving boundary value problems of partial differential equations or systems of such equations, on such region, using solutions of that differential equations or its adjoint, defined in its subregions*. With this method the solution domain Ω is subdivided into elements, and over each element e, the assumed intraelement fields are

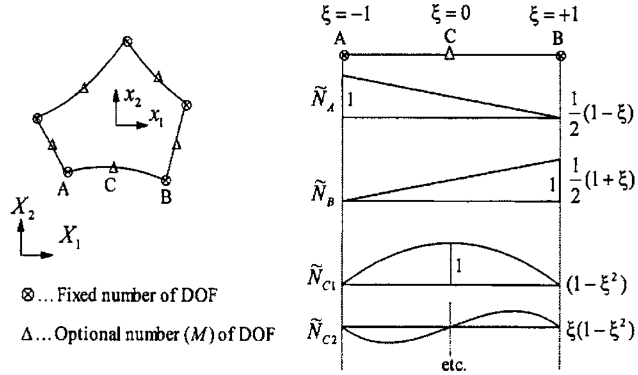

Fig. 1 Configuration of the T-element model

$$\mathbf{u}=\breve{\mathbf{u}}+\sum_{i=1}^{m}\mathbf{N}_i\mathbf{c}_i=\breve{\mathbf{u}}+\mathbf{N}\mathbf{c} \tag{9}$$

where $\breve{\mathbf{u}}$ and $\mathbf{N}_i$ are known functions and $\mathbf{c}_i$ is a coefficient vector. If the governing differential equations are written as

$$\Re\mathbf{u}(\mathbf{x})=\bar{\mathbf{b}}(\mathbf{x}), \quad (\mathbf{x}\in\Omega_e) \tag{10}$$

where $\Re$ stands for the differential operator matrix, $\mathbf{x}$ for the position vector, the overhead bar indicates the imposed quantities, and Ω_e stands for the eth element subdomain, then $\breve{\mathbf{u}}=\breve{\mathbf{u}}(\mathbf{x})$ and $\mathbf{N}_i=\mathbf{N}_i(\mathbf{x})$ in Eq. (9) have to be chosen such that

$$\Re\breve{\mathbf{u}}=\bar{\mathbf{b}} \quad \text{and} \quad \Re\mathbf{N}_i=0, \quad (i=1,2,\cdots,m) \tag{11}$$

everywhere in Ω_e. The unknown coefficient $\mathbf{c}$ may be calculated from the conditions on the external boundary and/or the continuity conditions on the interelement boundary. Thus various Trefftz-element models can be obtained by using different approaches to enforce these conditions. In the majority of approaches, a hybrid technique is usually used whereby the elements are linked through an auxiliary conforming displacement frame, which has the same form as in conventional FE method. This means that, in the Trefftz FE approach, a conforming potential (or displacement in solid mechanics) field should be independently defined on the element boundary to enforce the potential continuity between elements and also to link the coefficient $\mathbf{c}$, appearing in Eq. (9), with nodal displacement $\mathbf{d}(=\{d\})$. The frame is defined as

$$\tilde{\mathbf{u}}(\mathbf{x})=\tilde{\mathbf{N}}(\mathbf{x})\mathbf{d}, \quad (\mathbf{x}\in\Gamma_e) \tag{12}$$

where the symbol "$\sim$" is used to specify that the field is defined on the element boundary only, $\mathbf{d}=\mathbf{d}(\mathbf{c})$ stands for the vector of the nodal displacements, which are the final unknowns of the problem, Γ_e represents the boundary of element e, and $\tilde{\mathbf{N}}$ is a matrix of the corresponding shape functions, typical examples of which are displayed in Fig. 1.

2.3 T-Complete Functions. T-complete functions, also called Trefftz functions, are very important in deriving Trefftz element formulation. For this reason it is necessary to know how to construct them and what is the suitable criterion for completeness. The proof of completeness, as well as its general procedures, can be found in the work of Colton [125], Henrici [126], and Herrera [127]. For illustration, let us consider the Laplace equation

$$\nabla^2 u=0 \tag{13}$$

where $\nabla^2=\partial^2/\partial x^2+\partial^2/\partial y^2$ is the two-dimensional Laplace operator. Its T-complete solutions are a series of functions satisfying Eq. (13) and being complete in the sense of containing all possible solutions in a given solution domain. It can be shown that any of the following functions satisfies Eq. (13):

$$1, r\cos\theta, \quad r\sin\theta, \cdots, \quad r^m\cos m\theta, \quad r^m \sin m\theta, \cdots \tag{14}$$

where r and θ are a pair of polar coordinates. As a consequence, the so-called T-complete set, denoted by $\mathbf{T}$, can be written as

$$\mathbf{T} = \{1, r^m\cos m\theta, r^m\sin m\theta\} = \{T_i\} \tag{15}$$

2.4 Variational Principles. The Trefftz FE equation for the boundary value problem (1)–(7) can be established by the variational approach [61]. Since the stationary conditions of the traditional potential and complementary variational functional may not satisfy the interelement continuity condition, which is required in Trefftz FE analysis, several variants of modified variational functionals have been used in the literature to establish Trefftz FE equation. We list here three of them that have been widely used in numerical analysis as below.

1. The two variational principles below were due to Herrera [75,82] and Herrera et al. [83] and are applicable to any boundary value problems. The first one is in terms of the "prescribed data"

$$\int_\Omega w\mathfrak{R}u dx - \int_\Gamma \aleph(u,w)dx - \int_\Sigma \mathfrak{T}(u,w)dx = \int_\Omega fw dx - \int_\Gamma gw dx - \int_\Sigma jw dx \quad \forall\, w \in D \tag{16}$$

while the second one is in terms of the "sought information"

$$\int_\Omega u\mathfrak{R}^* w dx - \int_\Gamma C^*(u,w)dx - \int_\Sigma K^*(u,w)dx = \int_\Omega fw dx - \int_\Gamma gw dx - \int_\Sigma jw dx \quad \forall\, w \in D \tag{17}$$

where $\mathfrak{R}^*$ is a formal adjoint of $\mathfrak{R}$ in an abstract sense defined in [82], $\aleph(u,w)$ and $C^*(u,w)$ are boundary operators, while $\mathfrak{T}(u,w)$ and $K^*(u,w)$ are, respectively, the jump and average operators, Σ stands for the internal boundary, f is body force, g is generalized boundary force, and j is the force related to discontinuities (see [75,82] for a more detailed explanation on these symbols). The variational principles (16) and (17) were called "direct" and "indirect" variational formulations of the original boundary value problem, respectively.

2. An alternative variational functional for hybrid-Trefftz displacement-type formulation is given by [30]

$$J(\mathbf{u},\tilde{\mathbf{v}}) = \sum_e \left(-\frac{1}{2}\int_{\Omega_e} \mathbf{u}_e^T \bar{\mathbf{b}} d\Omega - \frac{1}{2}\int_{\Gamma_e} \mathbf{t}_e^T \mathbf{v}_e ds + \int_{\Gamma_{e^*}} \mathbf{t}_e^T \tilde{\mathbf{v}}_e ds - \int_{\Gamma_{e\sigma}} \bar{\mathbf{t}}_e^T \tilde{\mathbf{v}}_e ds \right) = \text{stationary} \tag{18}$$

The boundary Γ_e of the element e consists of the following parts:

$$\Gamma_e = \Gamma_{eS} + \Gamma_{eu} + \Gamma_{e\sigma} + \Gamma_{Ie} = \Gamma_{eS} + \Gamma_{e^*} \tag{19}$$

in which Γ_{eS} is the portion of Γ_e on which the prescribed boundary conditions are satisfied a priori (this is the case when the special purpose trial functions are used in the element), Γ_{eu} and $\Gamma_{e\sigma}$ are portions of the remaining part, $\Gamma_e - \Gamma_{eS}$, of the element boundary on which either displacement ($\mathbf{v}=\bar{\mathbf{v}}$) or traction ($\mathbf{t}=\bar{\mathbf{t}}$) is prescribed, while Γ_{Ie} is the interelement portion of Γ_e.

3. The following modified variational functional will be used throughout this paper [61]:

$$\Pi_m = \sum_e \Pi_{me} = \sum_e \left[\Pi_e + \int_{\Gamma_{te}} (\bar{\mathbf{t}} - \mathbf{t})\tilde{\mathbf{u}} ds - \int_{\Gamma_{Ie}} \mathbf{t}\tilde{\mathbf{u}} ds \right] \tag{20}$$

$$\Psi_m = \sum_e \Psi_{me} = \sum_e \left[\Psi_e + \int_{\Gamma_{ue}} (\bar{\mathbf{u}} - \tilde{\mathbf{u}})\mathbf{t} ds - \int_{\Gamma_{Ie}} \mathbf{t}\tilde{\mathbf{u}} ds \right] \tag{21}$$

where

$$\Pi_e = \int\int_{\Omega_e} \Pi(\boldsymbol{\sigma}) d\Omega - \int_{\Gamma_{ue}} \mathbf{t}\bar{\mathbf{u}} ds \tag{22}$$

$$\Psi_e = \int\int_{\Omega_e} [\Psi(\boldsymbol{\varepsilon}) - \bar{\mathbf{b}}\mathbf{u}] d\Omega - \int_{\Gamma_{te}} \bar{\mathbf{t}}\tilde{\mathbf{u}} ds \tag{23}$$

with

$$\Pi(\boldsymbol{\sigma}) = \tfrac{1}{2}\boldsymbol{\sigma}^T \mathbf{C}\boldsymbol{\sigma}, \quad \Psi(\varepsilon) = \tfrac{1}{2}\boldsymbol{\varepsilon}^T \mathbf{D}\boldsymbol{\varepsilon} \tag{24}$$

in which $\mathbf{C}=\mathbf{D}^{-1}$ and Eq. (1) are assumed to be satisfied a priori. The term "modified principle" refers here to the use of a conventional functional and some modified terms for the construction of a special variational principle to account for additional requirements, such as the condition defined in Eqs. (6) and (7).

The boundary Γ_e of a particular element consists of the following parts:

$$\Gamma_e = \Gamma_{ue} \cup \Gamma_{te} \cup \Gamma_{Ie} \tag{25}$$

where

$$\Gamma_{ue} = \Gamma_u \cap \Gamma_e, \quad \Gamma_{te} = \Gamma_t \cap \Gamma_e, \tag{26}$$

and Γ_{Ie} is the interelement boundary of the element e. The stationary condition of the functional (20) or (21) and the theorem on the existence of extremum of the functional, which ensures that an approximate solution can converge to the exact one, was discussed by Qin [61].

2.5 Generation of Element Stiffness Matrix. The element matrix equation can be generated by setting $\delta\Pi_{me}=0$ or $\delta\Psi_{me}=0$. By reason of the solution properties of the intraelement trial functions, the functional Π_{me} in Eq. (20) can be simplified to

$$\Pi_{me} = \frac{1}{2}\int_{\Omega_e} \mathbf{u}\bar{\mathbf{b}} d\Omega + \frac{1}{2}\int_{\Gamma_e} \mathbf{t}\mathbf{u} ds + \int_{\Gamma_{te}} (\bar{\mathbf{t}} - \mathbf{t})\tilde{\mathbf{u}} ds - \int_{\Gamma_{Ie}} \mathbf{t}\tilde{\mathbf{u}} ds - \int_{\Gamma_{ue}} \mathbf{t}\bar{\mathbf{u}} ds \tag{27}$$

Substituting the expressions given in Eqs. (9) and (12) into (20) and using Eqs. (2), (3), and (5) produces

$$\Pi_{me} = -\tfrac{1}{2}\mathbf{c}^T\mathbf{H}\mathbf{c} + \mathbf{c}^T\mathbf{S}\mathbf{d} + \mathbf{c}^T\mathbf{r}_1 + \mathbf{d}^T\mathbf{r}_2 + \text{terms without } \mathbf{c} \text{ or } \mathbf{d} \tag{28}$$

in which the matrices $\mathbf{H}, \mathbf{S}$ and the vectors $\mathbf{r}_1, \mathbf{r}_2$ are all known [61].

To enforce interelement continuity on the common element boundary, the unknown vector $\mathbf{c}$ should be expressed in terms of nodal degrees of freedom $\mathbf{d}$. An optional relationship between $\mathbf{c}$ and $\mathbf{d}$ in the sense of variation can be obtained from

$$\frac{\partial \Pi_{me}}{\partial \mathbf{c}^T} = -\mathbf{H}\mathbf{c} + \mathbf{S}\mathbf{d} + \mathbf{r}_1 = 0 \tag{29}$$

This leads to

$$\mathbf{c} = \mathbf{G}\mathbf{d} + \mathbf{g} \tag{30}$$

where $\mathbf{G}=\mathbf{H}^{-1}\mathbf{S}$ and $\mathbf{g}=\mathbf{H}^{-1}\mathbf{r}_1$, and then straightforwardly yields the expression of Π_{me} only in terms of $\mathbf{d}$ and other known matrices

$$\Pi_{me} = \frac{1}{2}\mathbf{d}^T\mathbf{G}^T\mathbf{H}\mathbf{G}\mathbf{d} + \mathbf{d}^T(\mathbf{G}^T\mathbf{H}\mathbf{g} + \mathbf{r}_2) + \text{terms without } \mathbf{d} \tag{31}$$

Therefore, the element stiffness matrix equation can be obtained by taking the vanishing variation of the functional Π_{me} as

$$\frac{\partial \Pi_{me}}{\partial \mathbf{d}^T} = 0 \Rightarrow \mathbf{K}\mathbf{d} = \mathbf{P} \tag{32}$$

where $\mathbf{K}=\mathbf{G}^T\mathbf{H}\mathbf{G}$ and $\mathbf{P}=-\mathbf{G}^T\mathbf{H}\mathbf{g}-\mathbf{r}_2$ are, respectively, the element stiffness matrix and the equivalent nodal flow vector. The expression (32) is the elemental stiffness matrix equation for Trefftz FE analysis.

3 Potential Problems

This section is concerned with the application of the HT FE to the solution of steady potential flow problems. By steady potential problems we mean those governed by the Laplace, Poisson, or Helmholtz equations. The method presented is based on a modified variational principle and the T-complete functions discussed in Sec. 2.

3.1 Basic Equations and Assumed Fields. Consider that we are seeking to find the solution of a Poisson (or Laplace for $\bar{b}=0$ below) equation in a domain Ω

$$\nabla^2 u = \bar{b} \quad (\text{in } \Omega) \tag{33}$$

with $\bar{b}$ a known function and with boundary conditions

$$u = \bar{u} \quad (\text{on } \Gamma_u) \tag{34}$$

$$q_n = \frac{\partial u}{\partial n} = \bar{q}_n \quad (\text{on } \Gamma_q) \tag{35}$$

where n is the normal to the boundary, $\Gamma=\Gamma_u+\Gamma_q$ and the dashes indicate that those variables are known.

By way of the method of variable separation, the complete solutions in a bounded region are obtained as [43]

$$u(r,\theta) = \sum_{m=0}^{\infty} r^m(a_m \cos m\theta + b_m \sin m\theta) \tag{36}$$

for two-dimensional problems and

$$u(r,\theta) = \sum_{m=0}^{\infty} a_m r^m P_m^q(\cos\theta)e^{iq\phi} \tag{37}$$

for three-dimensional problems, where $P_m^q(\cos\theta)$ is the associated Legendre function, $-m \leqslant q \leqslant m$, and the spherical coordinates (r,θ,ϕ) are used in Eq. (37). The complete solutions in an unbounded region can be similarly obtained [61]. Thus, the associated T-complete sets of Eqs. (36) and (37) can be expressed in the form

$$\mathbf{T} = \{1, r^m \cos m\theta, r^m \sin m\theta\} = \{T_i\} \tag{38}$$

$$\mathbf{T} = \{r^m P_m^q(\cos\theta)e^{iq\phi}\} = \{T_i\} \tag{39}$$

The internal trial function N_j $(j=1,2\ldots m)$ in Eq. (9) are in this case obtained by a suitably truncated T-complete solution (38) or (39). For example,

$$N_1 = r\cos\theta, \quad N_2 = r\sin\theta, \quad N_3 = r^2\cos 2\theta, \ldots, \tag{40}$$

for a two-dimensional problem with a bounded domain. Note that the function $N_1=1$ is not used here, as it represents rigid body motion and yields zero element stiffness (this is discussed, in detail, in Sec. 3.7). The particular solution $\breve{u}$ for any right-hand side $\bar{b}$ can be obtained by integration of the source (or Green's) function [61]

$$u^*(r_{PQ}) = \frac{1}{2\pi}\ln\left(\frac{1}{r_{PQ}}\right) \tag{41}$$

where P designates the field point under consideration, Q stands for the source point, and

$$r_{PQ} = \sqrt{(x_Q - x_P)^2 + (y_Q - y_P)^2} \tag{42}$$

The Green's function $u^*(r_{PQ})$ is the solution for the Laplace equation in an infinite domain and with a unit potential applied at a given point Q, i.e.,

$$\nabla^2 u^* = \delta(P,Q) \tag{43}$$

where $\delta(P,Q)$ is a Dirac δ function representing a unit concentrated potential acting at a point Q. As a consequence, the particular solution $\breve{u}$ in Eq. (9) can be expressed as

$$\breve{u}(P) = \frac{1}{2\pi}\int_{\Omega_e} \bar{b}(Q)\ln\left(\frac{1}{r_{PQ}}\right)d\Omega(Q) \tag{44}$$

The corresponding outward normal derivative of u ("traction") on Γ_e of element e is

$$t = q_n = \frac{\partial u}{\partial n} = \breve{q}_n + \sum_{j=1}^{m} T_j c_j = \breve{q}_n + \mathbf{Q}\mathbf{c} \tag{45}$$

3.2 Modified Variational Principle and Element Matrix Equation. The HT FE for potential problems can be established by means of a modified variational functional (which is slightly different from that of Chap. 2 in [61])

$$\Pi_{me} = -\frac{1}{2}\int_{\Omega} \bar{b}u\,d\,\Omega + \frac{1}{2}\int_{\Gamma_e} q_n u ds - \int_{\Gamma_{eu}} q_n \bar{u} ds + \int_{\Gamma_{eq}} (\bar{q}_n - q_n)\tilde{u} ds - \int_{\Gamma_{Ie}} q_n \tilde{u} ds \tag{46}$$

where $\Gamma_e=\Gamma_{eu}+\Gamma_{eq}+\Gamma_{Ie}$, with $\Gamma_{eu}=\Gamma_e\cap\Gamma_u$, $\Gamma_{eq}=\Gamma_e\cap\Gamma_q$, and Γ_{Ie} is the interelement boundary of element e. Substituting the expressions given in Eqs. (9), (12), and (45) into (46) yields Eq. (28). The matrices $\mathbf{H},\mathbf{S}$ and the vectors $\mathbf{r}_1,\mathbf{r}_2$ appeared in Eq. (28) are now defined by

$$\mathbf{H} = -\int_{\Gamma_e} \mathbf{Q}^T\mathbf{N} ds \tag{47}$$

$$\mathbf{S} = -\int_{\Gamma_{Ie}} \mathbf{Q}^T\tilde{\mathbf{N}} ds - \int_{\Gamma_{eq}} \mathbf{Q}^T\tilde{\mathbf{N}} ds \tag{48}$$

$$\mathbf{r}_1 = -\frac{1}{2}\int_{\Omega_e} \mathbf{N}^T\bar{b}d\Omega + \frac{1}{2}\int_{\Gamma_e} (\breve{q}_{ne}\mathbf{N}^T + \mathbf{Q}^T\breve{u}_e)ds - \int_{\Gamma_{eu}} \mathbf{Q}^T\bar{u} ds \tag{49}$$

$$\mathbf{r}_2 = -\int_{\Gamma_{Ie}} \tilde{\mathbf{N}}^T\breve{q}_{ne} ds + \int_{\Gamma_{eq}} \tilde{\mathbf{N}}^T(\bar{q}_n - \breve{q}_{ne})ds \tag{50}$$

The element stiffness matrix equation is the same as Eq. (32).

3.3 Special Purpose Functions. Singularities induced by local defects, such as angular corners, cracks, etc., can be accurately accounted for in the conventional FE model by way of appropriate

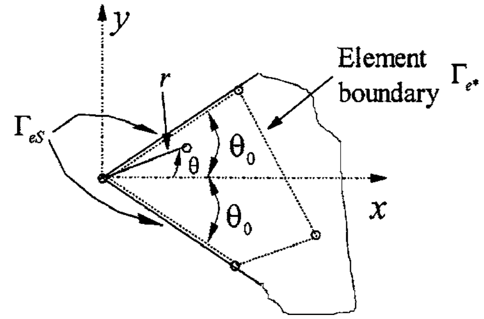

Fig. 2 Special element containing a singular corner

local refinement of the element mesh. However, an important feature of the Trefftz FE method is that such problems can be far more efficiently handled by the use of special purpose functions [30]. Elements containing local defects (see Fig. 2) are treated by simply replacing the standard regular functions **N** in Eq. (9) by appropriate special-purpose functions. One common characteristic of such trial functions is that it is not only the governing differential equations, which are Poisson equations here, which are satisfied exactly, but also some prescribed boundary conditions at a particular portion Γ_{eS} (see Fig. 2) of the element boundary. This enables various singularities to be specifically taken into account without troublesome mesh refinement. Since the whole element formulation remains unchanged (except that now the frame function $\tilde{\mathbf{u}}$ in Eq. (12) is defined and the boundary integration is performed at the portion Γ_{e^*} of the element boundary $\Gamma_e=\Gamma_{e^*}+\Gamma_{eS}$ only, see Fig. 2), all that is needed to implement the elements containing such special trial functions is to provide the element subroutine of the standard, regular elements with a library of various optional sets of special purpose functions.

The special purpose functions for such a singular corner has been given (p. 56 in [61]) as

$$u(r,\theta) = a_0 + \sum_{n=1}^{\infty} a_n r^{n\pi/\theta_0} \cos\left(\frac{n\pi}{\theta_0}\theta\right) + \sum_{n=1,3,5}^{\infty} d_n r^{n\pi/2\theta_0} \sin\left(\frac{n\pi}{2\theta_0}\theta\right) \tag{51}$$

3.4 Orthotropic Case. Consider the case of an orthotropic body as shown in Fig. 3. The equilibrium equation in the directions of orthotropy can be written as

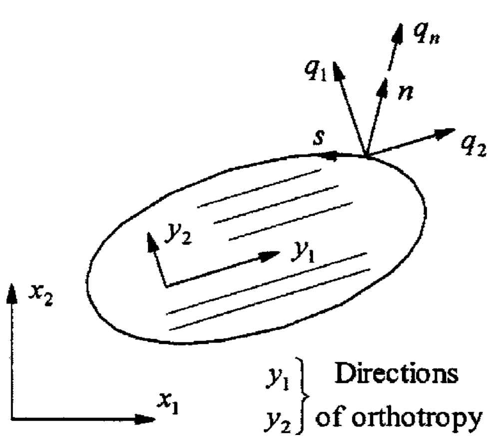

Fig. 3 Orthotropic configuration of potential problem

$$k_1 \frac{\partial^2 u}{\partial y_1^2} + k_2 \frac{\partial^2 u}{\partial y_2^2} = 0 \tag{52}$$

for the two-dimensional case, where k_i is the medium property coefficient in the direction of orthotropy i. Note that y_i are the directions of orthotropy. The simplest way of finding the T-complete solutions of this problem is by using the transformation

$$z_i = \frac{y_i}{\sqrt{k_i}} \tag{53}$$

with which Eq. (52) can be rewritten as

$$\nabla_0^2 u = 0 \tag{54}$$

where $\nabla_0^2 = \partial^2/\partial z_1^2 + \partial^2/\partial z_2^2$.

Hence, we have the same forms of complete solution as in the isotropic case. They are

$$u(r,\theta) = \sum_{m=0}^{\infty} r^m (a_m \cos m\theta + b_m \sin m\theta) \tag{55}$$

where

$$r = (z_1^2 + z_2^2)^{1/2} = \left(\frac{y_1^2}{k_1} + \frac{y_2^2}{k_2}\right)^{1/2}, \quad \theta = \arctan\left(\frac{z_2}{z_1}\right) = \arctan\left(\frac{\sqrt{k_1} y_2}{\sqrt{k_2} y_1}\right) \tag{56}$$

The variational functional used to establish the element matrix equation of this problem has the same form as that of Eq. (46), except that the variables q_1 and q_2 are replaced by q_{z_1} and q_{z_2}, respectively, i.e.,

$$q_1 \Rightarrow q_{z_1} = \frac{\partial u}{\partial z_1} \quad \text{and} \quad q_2 \Rightarrow q_{z_2} = \frac{\partial u}{\partial z_2} \tag{57}$$

which gives

$$\Pi_{me} = \frac{1}{2}\int_{\Omega_e} (q_{z_1}^2 + q_{z_2}^2) d\Omega - \int_{\Gamma_{eu}} \bar{q}_n \tilde{u} ds + \int_{\Gamma_{eq}} (\bar{q}_n - q_n) \tilde{u} ds - \int_{\Gamma_{el}} q_n \tilde{u} ds \tag{58}$$

3.5 The Helmholtz Equation. Another interesting potential problem type that can be solved using the Trefftz FE approach is the case of the Helmholtz or wave equation. Its differential equation is

$$\nabla^2 u + \lambda^2 u = 0 \quad (\text{in } \Omega) \tag{59}$$

where λ^2 is a positive and known parameter. By using the method of variable separation, the complete solutions for the Helmholtz equation in two-dimensional bounded and unbounded regions can be obtained as [6]

$$u(r,\theta) = a_0 J_0(\lambda r) + \sum_{m=1}^{\infty} [a_m J_m^{(1)}(\lambda r) \cos m\theta + b_m J_m^{(1)}(\lambda r) \sin m\theta] \tag{60}$$

for a bounded region, and

$$u(r,\theta) = a_0 J_0(\lambda r) + \sum_{m=1}^{\infty} [a_m H_m^{(1)}(\lambda r) \cos m\theta + b_m H_m^{(1)}(\lambda r) \sin m\theta] \tag{61}$$

for an unbounded region, and the corresponding T-complete sets of solutions of Eqs. (60) and (61) can be taken as

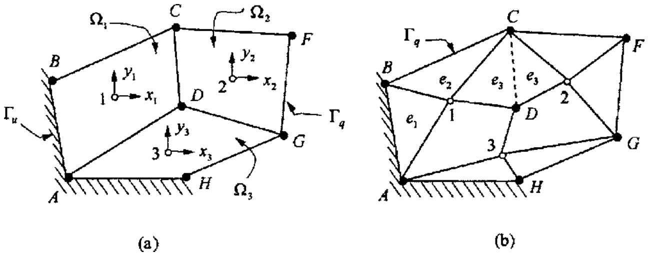

Fig. 4 FE version of approach: (*a*) subdivision into subdomains $\Omega_1, \Omega_2, \ldots$ with piecewise approximations $u_1, u_2, \ldots$; and (*b*) corresponding FE mesh with nodes 1,2,…etc.

$$\mathrm{T} = \{J_0(\lambda r), J_m(\lambda r)\cos m\theta, J_m(\lambda r)\sin m\theta\} = \{T_i\} \tag{62}$$

$$\mathrm{T} = \{H_0^{(1)}(\lambda r), H_m^{(1)}(\lambda r)\cos m\theta, H_m^{(1)}(\lambda r)\sin m\theta\} = \{T_i\} \tag{63}$$

in which $J_m(\lambda r)$ and $H_m^{(1)}(\lambda r)$ are the Bessel and Hankel functions of the first kind, respectively. As an illustration, the internal function N_j in Eq. (9) can be given in the form

$$N_1 = J_0(\lambda r), \quad N_2(\lambda r) = J_1(\lambda r)\cos\theta, \quad N_3 = J_1(\lambda r)\sin\theta, \cdots \tag{64}$$

for two-dimensional Helmholtz equations with bounded regions. For a particular element, say element e, the variational functional used for generating the element matrix equation of this problem is

$$\Pi_{me} = \frac{1}{2}\int_{\Omega_e}(q_1^2 + q_2^2 - \lambda^2 u^2)d\Omega - \int_{\Gamma_{eu}}\tilde{q}_n\bar{u}ds + \int_{\Gamma_{eq}}(\bar{q}_n - q_n)\tilde{u}ds - \int_{\Gamma_{el}} q_n\tilde{u}ds \tag{65}$$

Before concluding this subsection, we would like to mentioned that, for Helmholtz equation, Sanchez et al. [128] have shown that a suitable system of plane waves is TH-complete in any bounded region. This is a TH-complete system which, because of its simplicity, could be advantageously used for implementing Trefftz method.

3.6 Frameless Trefftz Elements. As opposed to the hybrid approach, which makes use of the independently defined auxiliary inter-element frame, the frameless T-element approach is based on the least-squares formulation and was recently presented by Jirousek and Wroblewski [9]. Jirousek and Stojek [42], and Stojek [89]. This approach is based on the application of a suitably truncated T-complete set (38) over individual subdomains linked by means of a least-squares procedure. This section describes some aspects of the approach in order to provide a brief introduction to the concept of frameless Trefftz elements.

Consider again a two-dimensional Poisson equation problem

$$\nabla^2 u = \bar{b} \ (\text{in } \Omega), \quad u = \bar{u} \ (\text{on } \Gamma_u), \quad q_n = \frac{\partial u}{\partial n} = \bar{q} \ (\text{on } \Gamma_q) \tag{66}$$

The solution domain Ω (Fig. 4) is divided into subdomains, $\Omega = \cup_e \Omega_e$, and over each Ω_e the potential u is approximated by the expansion (9). Moreover, to prevent numerical problems, the trial functions must be defined in terms of the local coordinates as shown in Fig. 4(*a*).

The functional to be minimized enforces in the least-squares sense the boundary conditions on $\Gamma_u \cup \Gamma_q$ and the continuity in potential u and reciprocity of the boundary flux on all subdomain interfaces Γ_l

$$I(\mathbf{c}) = \int_{\Gamma_u}(u - \bar{u})^2 ds + w^2\int_{\Gamma_q}(q_n - \bar{q}_n)^2 ds + \int_{\Gamma_l}[(u^+ - u^-)^2 + w^2(q_n^+ + q_n^-)^2]ds = \min \tag{67}$$

where $\mathbf{c} = \{\mathbf{c}_1, \mathbf{c}_2, \ldots\}$, the plus and minus superscripts designate solutions from any two neighboring Trefftz fields along Γ_l, and w is some positive weight coefficient, which serves the purpose of restoring the homogeneity of physical dimensions and tuning the strength laid on the potential and flux conditions, respectively. For the solution domain shown in Fig. 4, the boundaries Γ_l, Γ_u, and Γ_q in Eq. (67) are given as follows:

$$\Gamma_l = \Gamma_{DA} \cup \Gamma_{DC} \cup \Gamma_{DG}, \quad \Gamma_u = \Gamma_{HA} \cup \Gamma_{AB}, \quad \Gamma_q = \Gamma_{BC} \cup \Gamma_{CF} \cup \Gamma_{FG} \cup \Gamma_{GH} \tag{68}$$

The vanishing variation of I may be written as

$$\delta I = \delta\mathbf{c}^T\frac{\partial I}{\partial \mathbf{c}} = \delta\mathbf{c}^T(\mathbf{K}\mathbf{c} + \check{\mathbf{r}}) = 0 \tag{69}$$

which yields for the unknown $\mathbf{c}$ of the whole assembly of subdomains the following symmetric system of linear equations:

$$\mathbf{K}\mathbf{c} + \check{\mathbf{r}} = 0 \tag{70}$$

3.7 Rank Condition. By checking the functional (46), we know that the solution fails if any of the functions N_j in u is a rigid-body motion mode associated with a vanishing boundary flux term of the vector $\mathbf{Q}$ in Eq. (45). As a consequence, the matrix $\mathbf{H}$ defined in Eq. (47) is not in full rank and becomes singular for inversion. Therefore, special care should be taken to discard from u all rigid-body motion terms and to form the vector $\mathbf{N} = \{N_1, N_2, \ldots, N_m\}$ as a set of linearly independent functions N_j associated with nonvanishing potential derivatives. Note that once the solution of the FE assembly has been performed, the missing rigid-body motion modes may, however, be easily recovered, if desired. It suffices to reintroduce the discarded modes in the internal field u of a particular element and then to calculate their undetermined coefficients by requiring, for example, the least-squares adjustment of u and $\tilde{u}$. The detailed procedure is given by Jirousek and Guex [30].

Furthermore, for a successful solution it is important to choose the proper number m of trial functions N_j for the element. The basic rule used to prevent spurious energy modes is analogous to that in the hybrid-stress model. The necessary (but not sufficient) condition for the matrix $\mathbf{H}$ to have full rank is stated as [30]

$$m \geqslant k - r \tag{71}$$

where k and r are numbers of nodal degrees of freedom of the element under consideration and of the discarded rigid-body motion terms. Though the use of the minimum number $m = k - r$ of flux mode terms in Eq. (9) does not always guarantee a stiffness matrix with full rank, full rank may always be achieved by suitably augmenting m. The optimal value of m for a given type of element should be found by numerical experimentation.

4 Plane Elasticity

This section deals with HT FE theory in linear elasticity. The small strain theory of elasticity is assumed [129–131] and developments of Trefftz-element formulation in plane elasticity are reviewed.

In this application, the intraelement field (9) becomes

$$\mathbf{u} = \begin{Bmatrix} u_1 \\ u_2 \end{Bmatrix} = \begin{Bmatrix} \check{u}_1 \\ \check{u}_2 \end{Bmatrix} + \sum_{j=1}^{m}\mathbf{N}_j\mathbf{c}_j = \check{\mathbf{u}} + \mathbf{N}\mathbf{c} \tag{72}$$

where $\mathbf{c}_j$ are undetermined coefficients and the known coordinate functions $\check{\mathbf{u}}$ and $\mathbf{N}_j$ are, respectively, particular integral and a set of appropriate homogeneous solutions to the equation

$$\mathbf{LDL}^T\breve{\mathbf{u}} + \bar{\mathbf{b}} = 0 \quad (\text{on } \Omega_e) \tag{73}$$

and

$$\mathbf{LDL}^T\mathbf{N}_j = 0 \quad (\text{on } \Omega_e) \tag{74}$$

where $\bar{\mathbf{b}}$, $\mathbf{L}$, and $\mathbf{D}$ are defined in Eq. (8) for plane stress problems. For plane strain applications, it suffices to replace E and μ above by

$$E^* = \frac{E}{1-\mu^2}, \quad \mu^* = \frac{\mu}{1-\mu} \tag{75}$$

In the presence of constant body forces ($\bar{b}_1$ and $\bar{b}_2$ being two constants), the particular solution is conveniently taken as

$$\breve{\mathbf{u}} = -\frac{1+\mu}{E}\begin{Bmatrix} \bar{b}_1 y^2 \\ \bar{b}_2 x^2 \end{Bmatrix} \tag{76}$$

The distribution of the frame (12) can now be written as

$$\tilde{u}_1 = \tilde{N}_A\tilde{u}_{1A} + \tilde{N}_B\tilde{u}_{1B} + \sum_{i=1}^{M} \delta^{i-1}\tilde{N}_{Ci}a_{Ci} \tag{77}$$

$$\tilde{u}_2 = \tilde{N}_A\tilde{u}_{2A} + \tilde{N}_B\tilde{u}_{2B} + \sum_{i=1}^{M} \delta^{i-1}\tilde{N}_{Ci}b_{Ci} \tag{78}$$

along a particular side A-C-B of an element (Fig. 1), where $\tilde{N}_A$, $\tilde{N}_B$ and $\tilde{N}_{Ci}$ are defined in Fig. 1, δ is a coefficient equal to either 1 or -1 according to the orientation of the side A-C-B (Fig. 1) in the global coordinate system (X_1, X_2)

$$\delta = \begin{cases} +1 & \text{if } X_{1B} - X_{1A} \leqslant X_{2B} - X_{2A} \\ -1 & \text{otherwise} \end{cases} \tag{79}$$

A T-complete set of homogeneous solutions $\mathbf{N}_j$ can be generated in a systematic way from Muskhelishvili's complex variable formulation [132]. They can be written as [25]

$$2G\mathbf{N}_{ej} = \begin{Bmatrix} \text{Re } Z_{1k} \\ \text{Im } Z_{1k} \end{Bmatrix} \text{ with } Z_{1k} = i\kappa z^k + kiz\bar{z}^{k-1} \tag{80}$$

$$2G\mathbf{N}_{ej+1} = \begin{Bmatrix} \text{Re } Z_{2k} \\ \text{Im } Z_{2k} \end{Bmatrix} \text{ with } Z_{2k} = \kappa z^k - kz\bar{z}^{k-1} \tag{81}$$

$$2G\mathbf{N}_{ej+2} = \begin{Bmatrix} \text{Re } Z_{3k} \\ \text{Im } Z_{3k} \end{Bmatrix} \text{ with } Z_{3k} = i\bar{z}^k \tag{82}$$

$$2G\mathbf{N}_{ej+3} = \begin{Bmatrix} \text{Re } Z_{4k} \\ \text{Im } Z_{4k} \end{Bmatrix} \text{ with } Z_{4k} = -\bar{z}^k \tag{83}$$

The corresponding stress field is obtained by the standard constitutive relation (2)

$$\boldsymbol{\sigma} = \begin{Bmatrix} \boldsymbol{\sigma}_{11} \\ \boldsymbol{\sigma}_{22} \\ \boldsymbol{\sigma}_{12} \end{Bmatrix} = \breve{\boldsymbol{\sigma}} + \sum_{j=1}^{m} \mathbf{T}_j\mathbf{c}_j = \breve{\boldsymbol{\sigma}} + \mathbf{Tc} \tag{84}$$

while the particular solution $\breve{\boldsymbol{\sigma}}$ can be easily obtained by setting $\breve{\boldsymbol{\sigma}} = \mathbf{DL}^T\breve{\mathbf{u}}$. Derivation of the element stiffness equation is based on the functional

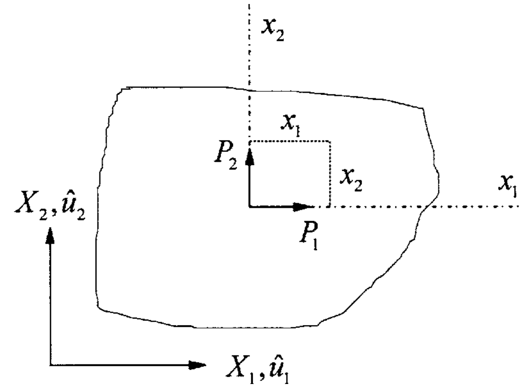

Fig. 5 Isolated concentrated loads in infinite plane

$$\Pi_{me} = \frac{1}{2}\int_{\Omega_e} (\mathbf{L}^T\mathbf{u})^T\mathbf{DL}^T\mathbf{u}\,d\Omega - \int_{\Gamma_{eu}} \tilde{\mathbf{t}}\tilde{\mathbf{u}}\,ds + \int_{\Gamma_{e\sigma}} (\bar{\mathbf{t}} - \mathbf{t})\tilde{\mathbf{u}}\,ds - \int_{\Gamma_{el}} \mathbf{t}\tilde{\mathbf{u}}\,ds \tag{85}$$

Let us turn our attention to discuss two representative special-purpose element models. First, we consider a concentrated load acting at a point of any element (Fig. 5). Singularities produced by the load can accurately be accounted for by augmenting the particular solution $\breve{\mathbf{u}}_e$ with the suitable singular solution $\hat{\mathbf{u}}_e$. For an isolated force in an infinite plane, for example (Fig. 5), the plane stress solution [133] yields the following displacements:

$$\hat{u}_1 = \frac{1+\mu}{4\pi E}P_1\left[(1+\mu)\frac{x_1^2}{r^2} - \frac{3-\mu}{2}\ln\frac{r^2}{l^2}\right] + \frac{(1+\mu)^2}{4\pi E}P_2\frac{x_1x_2}{r^2} \tag{86}$$

$$\hat{u}_2 = \frac{(1+\mu)^2}{4\pi E}P_1\frac{x_1x_2}{r^2} + \frac{1+\mu}{4\pi E}P_2\left[(1+\mu)\frac{x_2^2}{r^2} - \frac{3-\mu}{2}\ln\frac{r^2}{l^2}\right] \tag{87}$$

where $l > 0$ is an arbitrary positive constant used to give a reference frame, $r^2 = x_1^2 + x_2^2$, and P_1 and P_2 are the values of concentrated loads shown in Fig. 5.

Another special-purpose element model is concerned with a singular corner (Fig. 6). A complete set of Trefftz functions verifying the free stress conditions along the sides of a notch can be obtained by using the Williams' eigenfunctions [134]. Such func-

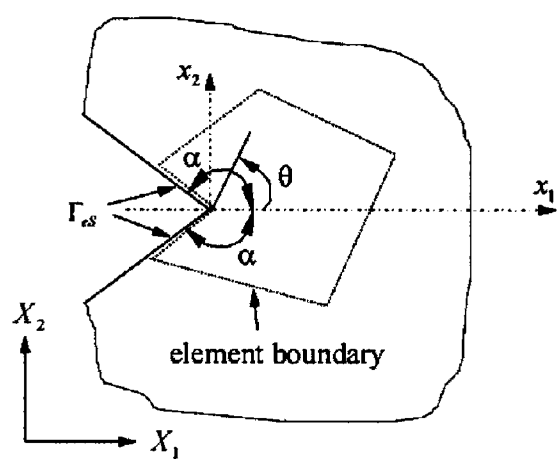

Fig. 6 Singular V-notched element

tions have, in the past, been used successfully by Lin and Tong [135] to generate a singular V-notched superelement. These functions can be used to generate special-purpose elements with singular corners. They are

$$2Gu_1 = a\sum_n \mathrm{Re}\left\{\left(\frac{r}{a}\right)^{\lambda_n}\beta_n[(\kappa+\lambda_n\cos 2\alpha+\cos 2\lambda_n\alpha)\cos\lambda_n\theta - \lambda_n\cos(\lambda_n-2)\theta] - \left(\frac{r}{a}\right)^{\zeta_n}\eta_n[(\kappa+\zeta_n\cos 2\alpha-\cos 2\zeta_n\alpha)\times\sin\zeta_n\theta-\zeta_n\sin(\zeta_n-2)\theta]\right\} \tag{88}$$

$$2Gu_2 = a\sum_n \mathrm{Re}\left\{\left(\frac{r}{a}\right)^{\lambda_n}\beta_n[(\kappa-\lambda_n\cos 2\alpha-\cos 2\lambda_n\alpha)\sin\lambda_n\theta + \lambda_n\sin(\lambda_n-2)\theta] + \left(\frac{r}{a}\right)^{\zeta_n}\eta_n[(\kappa-\zeta_n\cos 2\alpha+\cos 2\zeta_n\alpha)\times\cos\zeta_n\theta+\zeta_n\cos(\zeta_n-2)\theta]\right\} \tag{89}$$

where a is defined by

$$a = \sum_{i=1}^{N}\frac{(x_{1i}^2+x_{2i}^2)^{1/2}}{N} \tag{90}$$

with N being the number of nodes in the element under consideration, β_n and η_n are real undetermined constants, α and θ are shown in Fig. 6, while λ_n and ζ_n are eigenvalues that have a real part greater than or equal to 1/2 and are the roots of the following characteristic equations:

$$\sin 2\lambda_n\alpha = -\lambda_n\sin 2\alpha \tag{91}$$

for symmetric (tension) loading, and

$$\sin 2\zeta_n\alpha = \zeta_n\sin 2\alpha \tag{92}$$

for antisymmetric (pure shear) loading.

Apart from their high efficiency in solving singular corner problems, the great advantage of the above special-purpose function set is the attractive possibility of straightforwardly evaluating the stress intensity factors K_I (opening mode) and K_{II} (sliding mode) from the first two internal parameters β_1 and η_1

$$K_I = \sqrt{2\pi}\lambda_1 a^{1-\lambda_1}(\lambda_1+1-\lambda_1\cos 2\alpha-\cos 2\lambda_1\alpha)\beta_1 \tag{93}$$

$$K_{II} = \sqrt{2\pi}\zeta_1 a^{1-\zeta_1}(\zeta_1-1-\zeta_1\cos 2\alpha+\cos 2\zeta_1\alpha)\eta_1 \tag{94}$$

5 Thin Plate Bending

In Secs 3 and 4, applications of Trefftz-elements to the potential problem and plane elasticity were reviewed. Extension of the procedure to thin plate bending is briefly reviewed in this section.

For thin-plate bending the equilibrium equation and its boundary conditions are well established in the literature (e.g., [61]).

In the case of a thin-plate element the internal displacement field (9) becomes

$$w = \breve{w} + \sum_{j=1}^{m} N_j c_j = \breve{w} + \mathbf{Nc} \tag{95}$$

where w is the transverse deflection, $\breve{w}$ and N_j are known functions, which should be chosen so that

$$D\nabla^4\breve{w} = \bar{q} \quad \text{and} \quad \nabla^4 N_j = 0, \quad (j=1,2,\cdots,m) \tag{96}$$

everywhere in the element sub-domain Ω_e, where $\bar{q}$ is the distributed vertical load per unit area, $\nabla^4=\partial^4/\partial x_1^4+2\partial^4/\partial x_1^2\partial x_2^2+\partial^4/\partial x_2^4$ is the biharmonic operator, and $D=Et^3/12(1-\mu^2)$. In the hybrid approach under consideration, the elements are linked through an auxiliary displacement frame

$$\tilde{\mathbf{v}} = \begin{Bmatrix}\tilde{w}\\ \tilde{w}_{,n}\end{Bmatrix} = \begin{bmatrix}\tilde{\mathbf{N}}_1\\ \tilde{\mathbf{N}}_2\end{bmatrix}\mathbf{d} = \tilde{\mathbf{N}}\mathbf{d} \tag{97}$$

where $\mathbf{d}$ stands for the vector of nodal parameters and $\tilde{\mathbf{N}}$ is the conventional finite element interpolating matrix such that the corresponding nodal parameters of the adjacent elements are matched. Based on the approach of variable separation, the T-complete solution of the biharmonic equation, $D\nabla^4 w=\bar{q}$, can be found [108,127]

$$w = \sum_{n=0}^{\infty}\{\mathrm{Re}[(a_n+r^2b_n)z^n]+\mathrm{Im}[(c_n+r^2d_n)z^n]\} \tag{98}$$

where

$$r^2 = x_1^2+x_2^2, \quad z = x_1+ix_2 \tag{99}$$

Hence, the T-complete system for plate-bending problems can be taken as

$$T = \{1, r^2, \mathrm{Re}\, z^2, \mathrm{Im}\, z^2, r^2\,\mathrm{Re}\, z, r^2\,\mathrm{Im}\, z, \mathrm{Re}\, z^3, \cdots\} \tag{100}$$

The Trefftz FE formulation for thin-plate bending can be derived by means of a modified variational principle (e.g., [22]). The related functional used for deriving the HT element formulation is constructed as

$$\Pi_m = \sum_e\left[\Pi_e - \int_{\Gamma_{e2}}(\bar{M}_n-M_n)\tilde{w}_{,n}ds + \int_{\Gamma_{e4}}(\bar{R}-R)\tilde{w}ds + \int_{\Gamma_{e5}}(M_n\tilde{w}_{,n}-R\tilde{w})ds\right] \tag{101}$$

where

$$\Pi_e = \int_{\Omega_e}Ud\Omega + \int_{\Gamma_{e1}}\tilde{M}_n\bar{w}_{,n}ds - \int_{\Gamma_{e3}}\tilde{R}\bar{w}ds \tag{102}$$

with

$$U = \frac{1}{2D(1-\mu^2)}[(M_{11}+M_{22})^2+2(1+\mu)(M_{12}^2-M_{11}M_{22})] \tag{103}$$

The boundary Γ_e of a particular element consists of the following parts:

$$\Gamma_e = \Gamma_{e1}+\Gamma_{e2}+\Gamma_{e5} = \Gamma_{e3}+\Gamma_{e4}+\Gamma_{e5} \tag{104}$$

where

$$\Gamma_{e1}=\Gamma_e\cap\Gamma_{w_n}, \Gamma_{e2}=\Gamma_e\cap\Gamma_M, \Gamma_{e3}=\Gamma_e\cap\Gamma_w, \Gamma_{e4}=\Gamma_e\cap\Gamma_R \tag{105}$$

and Γ_{e5} is the interelement boundary of the element.

The formulation described above can be extended to the case of thin plates on an elastic foundation. In this case, the left-hand side of the equation $D\nabla^4 w=\bar{q}$ and the related plate boundary equation, $M_n=M_{ij}n_in_j=\bar{M}_n$, must be augmented by the terms Kw and $-\alpha G_p w$, respectively:

$$D\nabla^4 w + Kw = \bar{q} \quad (\text{in } \Omega) \tag{106}$$

$$M_n = M_{ij}n_in_j - \alpha G_p w = \bar{M}_n \quad (\text{on } \Gamma_M) \tag{107}$$

where $\alpha=0$ for a Winkler-type foundation, $\alpha=1$ for a Pasternak-type foundation, and the reaction operator

$$K = \begin{cases} k_w & \text{for a Winkler-type foundation} \\ (k_p - G_p \nabla^2) & \text{for a Pasternak-type foundation} \end{cases} \tag{108}$$

with k_w being the coefficient of a Winkler-type foundation, and k_P and G_P being the coefficient and shear modulus of a Pasternak-type foundation. The T-complete functions for this problem are [61]

$$f(r,\theta) = a_0 f_0(r) + \sum_{m=1}^{\infty} [a_m f_m(r) \cos m\theta + b_m f_m(r) \sin m\theta] \tag{109}$$

where $f_m(r) = I_m(r\sqrt{C_2}) - J_m(r\sqrt{C_1})$ and the associated internal function N_j can be taken as

$$N_1 = f_0(r), \quad N_{2m} = f_m(r)\cos m\theta, \quad N_{2m+1} = f_m(r)\sin m\theta \quad (m = 1, 2, \cdots) \tag{110}$$

in which $I_m()$ and $J_m()$ are, respectively, modified and standard Bessel function of the first kind with order m, and

$$C_1 = C_2 = i\sqrt{k_w/D} \tag{111}$$

for a Winkler-type foundation, and

$$C_1 = -\frac{G_P}{2D} - \sqrt{\left(\frac{G_P}{2D}\right)^2 - \frac{k_P}{D}}, \quad C_2 = \frac{G_P}{2D} - \sqrt{\left(\frac{G_P}{2D}\right)^2 - \frac{k_P}{D}} \tag{112}$$

for a Pasternak-type foundation, and $i = \sqrt{-1}$.

The variational functional used for deriving HT FE formulation of thin plates on an elastic foundation has the same form as that of Eq. (101), except that the complementary energy density U in Eq. (103) is replaced by U^*

$$U^* = \frac{1}{2D(1-\mu^2)}[(M_{11} + M_{22})^2 + 2(1+\mu)(M_{12}^2 - M_{11}M_{22})] + V^* \tag{113}$$

where

$$V^* = \begin{cases} \dfrac{k_w w^2}{2} & \text{for a Winkler-type foundation} \\ \frac{1}{2}(k_P w^2 + G_P w_{,i} w_{,i}) & \text{for a Pasternak-type foundation} \end{cases} \tag{114}$$

6 Thick-Plate Problems

Based on the Trefftz method, Petrolito [37,38] presented a hierarchic family of triangular and quadrilateral Trefftz elements for analyzing moderately thick Reissner-Mindlin plates. In these HT formulations, the displacement and rotation components of the auxiliary frame field $\tilde{\mathbf{u}} = \{\tilde{w}, \tilde{\psi}_x, \tilde{\psi}_y\}^T$, used to enforce conformity on the internal Trefftz field $\mathbf{u} = \{w, \psi_x, \psi_y\}^T$, are independently interpolated along the element boundary in terms of nodal values. Jirousek et al. [34] showed that the performance of the HT thick-plate elements could be considerably improved by the application of a linked interpolation whereby the boundary interpolation of the displacement $\tilde{w}$ is linked through a suitable constraint with that of the tangential rotation component $\tilde{\psi}_s$. This concept, introduced by Xu [136], has been applied recently by several researchers to develop simple and well-performing thick-plate elements [33,34,137–140]. In contrast to thin-plate theory as described in the previous section, Reissner-Mindlin theory [141,142] incorporates the contribution of shear deformation to the transverse deflection. In Reissner-Mindlin theory, it is assumed that the transverse deflection of the middle surface is w, and that straight lines are initially normal to the middle surface rotate ψ_x about the y-axis and ψ_y about the x-axis. The variables (w, ψ_x, ψ_y) are considered to be independent variables and to be functions of x and y only. A convenient matrix form of the resulting relations of this theory may be obtained through use of the following matrix quantities:

$$\mathbf{u} = \{w, \psi_x, \psi_y\}^T \quad \text{(generalized displacement)} \tag{115}$$

$$\boldsymbol{\varepsilon} = \{\chi_x\ \chi_y\ \chi_{xy}\ \gamma_x\ \gamma_y\}^T = \mathbf{L}^T\mathbf{u} \quad \text{(generalized strains)} \tag{116}$$

$$\boldsymbol{\sigma} = \{-M_x - M_y - M_{xy}\ Q_x\ Q_y\}^T = \mathbf{D}\boldsymbol{\varepsilon} \quad \text{(generalized stresses)} \tag{117}$$

$$\mathbf{t} = \{Q_n - M_{nx} - M_{ny}\}^T = \mathbf{A}\boldsymbol{\sigma} \quad \text{(generalized boundary tractions)} \tag{118}$$

where $\mathbf{L}$, $\mathbf{D}$, and $\mathbf{A}$ are defined by

$$\mathbf{L} = \begin{bmatrix} 0 & 0 & 0 & \frac{\partial}{\partial x} & \frac{\partial}{\partial y} \\ \frac{\partial}{\partial x} & 0 & \frac{\partial}{\partial y} & -1 & 0 \\ 0 & \frac{\partial}{\partial y} & \frac{\partial}{\partial x} & 0 & -1 \end{bmatrix}, \quad \mathbf{A} = \begin{bmatrix} 0 & 0 & 0 & n_x & n_y \\ n_x & 0 & n_y & 0 & 0 \\ 0 & n_y & n_x & 0 & 0 \end{bmatrix},$$

$$\mathbf{D} = \begin{bmatrix} \mathbf{D}_M & 0 \\ 0 & \mathbf{D}_Q \end{bmatrix}$$

$$\mathbf{D}_M = \frac{Et^3}{12(1-\mu^2)} \begin{bmatrix} 1 & \mu & 0 \\ \mu & 1 & 0 \\ 0 & 0 & \frac{1-\mu}{2} \end{bmatrix}, \quad \mathbf{D}_Q = \frac{Etk}{2(1+\mu)} \begin{bmatrix} 1 & 0 \\ 0 & 1 \end{bmatrix} \tag{119}$$

with k being a correction factor for nonuniform distribution of shear stress across thickness t, which is usually taken as 5/6.

The governing differential equations of moderately thick plates are obtained if the differential equilibrium conditions are written in terms of $\mathbf{u}$ as

$$\mathbf{L}\boldsymbol{\sigma} = \mathbf{L}\mathbf{D}\mathbf{L}^T\mathbf{u} = \bar{\mathbf{b}} \tag{120}$$

where the load vector

$$\bar{\mathbf{b}} = \{\bar{q}\ \bar{m}_x\ \bar{m}_y\}^T \tag{121}$$

comprises the distributed vertical load in the z direction and the distributed moment loads about the y- and x-axes (the bar above the symbols indicates imposed quantities).

The corresponding boundary conditions are given by

a. *simply supported condition*

$$w = \bar{w} \ (\text{on } \Gamma_w), \quad \psi_s = \psi_i s_i = \bar{\psi}_s \ (\text{on } \Gamma_{\psi_s}), \quad M_n = M_{ij} n_i n_j = \bar{M}_n \ (\text{on } \Gamma_{M_n}) \tag{122}$$

b. *clamped condition*

$$w = \bar{w} \ (\text{on } \Gamma_w), \quad \psi_s = \bar{\psi}_s \ (\text{on } \Gamma_{\psi_s}), \quad \psi_n = \psi_i n_i = \bar{\psi}_n \ (\text{on } \Gamma_{\psi_n}) \tag{123}$$

c. *free-edge conditions*

Table 1 Examples of ordering of indexes *i*, *j*, and *k* appearing in Eqs. (137) and (138)

i	1	2	3	4	5	6	7	8	9	10	11	12	13	14	15	16	17
j	1	2	3	4	5	-	6	7	8	9	-	-	10	11	12	13	-
k	-	-	-	-	-	1	-	-	-	-	2	3	-	-	-	-	4
i	18	19	20	21	22	23	24	25	26	27	28	29	…	etc.			
j	-	14	15	16	17	-	-	18	19	20	21	-	…	etc.			
k	5	-	-	-	-	6	7	-	-	-	-	8	…	etc.			

$$M_n=\bar{M}_n \quad (\text{on } \Gamma_{M_n}), \quad M_{ns}=\bar{M}_{ns} \quad (\text{on } \Gamma_{M_{ns}}),$$

$$Q_n=Q_i n_i=\bar{Q}_n \quad (\text{on } \Gamma_Q) \tag{124}$$

where n and s are, respectively, unit vectors outward normal and tangent to the plate boundary $\Gamma(\Gamma=\Gamma_{\psi_n}\cup\Gamma_{M_n}=\Gamma_{\psi_s}\cup\Gamma_{M_{ns}}=\Gamma_w\cup\Gamma_Q)$.

The internal displacement field in a thick plate is given in Eq. (9), in which $\breve{\mathbf{u}}$ and $\mathbf{N}_j$ are, respectively, the particular and homogeneous solutions to the governing differential equations (120), namely,

$$\mathbf{LDL}^T\breve{\mathbf{u}}=\bar{\mathbf{b}} \quad \text{and} \quad \mathbf{LDL}^T\mathbf{N}_j=0, \quad (j=1,2,\cdots,m) \tag{125}$$

To generate the internal function $\mathbf{N}_j$, consider again the governing equations (120) and write them in a convenient form as

$$D\left[\frac{\partial^2\psi_x}{\partial x^2}+\frac{1-\mu}{2}\frac{\partial^2\psi_x}{\partial y^2}+\frac{1+\mu}{2}\frac{\partial^2\psi_y}{\partial x\,\partial y}\right]+C\left(\frac{\partial w}{\partial x}-\psi_x\right)=0 \tag{126}$$

$$D\left[\frac{\partial^2\psi_y}{\partial y^2}+\frac{1-\mu}{2}\frac{\partial^2\psi_y}{\partial x^2}+\frac{1+\mu}{2}\frac{\partial^2\psi_x}{\partial x\,\partial y}\right]+C\left(\frac{\partial w}{\partial y}-\psi_y\right)=0 \tag{127}$$

$$C\left(\nabla^2 w-\frac{\partial\psi_x}{\partial x}-\frac{\partial\psi_y}{\partial y}\right)=\bar{q} \tag{128}$$

where

$$D=\frac{Et^3}{12(1-\mu^2)}, \quad C\frac{5Et}{12(1+\mu)} \tag{129}$$

and where, for the sake of simplicity, vanishing distributed moment loads, $\bar{m}_x=\bar{m}_y=0$, have been assumed.

The coupling of the governing differential equations (126)–(128) makes it difficult to generate a T-complete set of homogeneous solutions for w, ψ_x, and ψ_y. To bypass this difficulty, two auxiliary functions f and g are introduced [143] such that

$$\psi_x=g_{,x}+f_{,y} \quad \text{and} \quad \psi_y=g_{,y}-f_{,x} \tag{130}$$

It should be pointed out that

$$g_{0,x}+f_{0,y}=0 \quad \text{and} \quad g_{0,y}-f_{0,x}=0 \tag{131}$$

are Cauchy-Riemann equations, the solution of which always exists. As a consequence, ψ_x and ψ_y remain unchanged if f and g in Eq. (130) are replaced by $f+f_0$ and $g+g_0$. This property plays an important part in the solution process. Using these two auxiliary functions, Eq. (126)–(128) is converted as the form

$$D\nabla^4 g=\bar{p} \quad \text{and} \quad \nabla^2 f-\lambda^2 f=0 \tag{132}$$

with $\lambda^2=10(1-\mu)/t^2$.

The relations (132) are the biharmonic equation and the modified Bessel equation, respectively. Their T-complete solutions are provided in Eq. (100) for the former and by Qin [61]

$$f_{2m}=I_m(\lambda r)\sin m\theta, \quad f_{2m+1}=I_m(\gamma r)\cos m\theta \quad (m=0,1,2,\cdots) \tag{133}$$

for the latter. Thus the series for f and g can be taken as

$$f_1=I_0(\lambda r), \quad f_{2k}=I_k(\lambda r)\cos k\theta, \quad f_{2k+1}=I_k(\lambda r)\sin k\theta \quad k=1,2,\ldots \tag{134}$$

$$g_1=r^2, \quad g_2=x^2-y^2, \quad g_3=xy, \quad g_{4k}=r^2\,\mathrm{Re}\,z^k$$

$$g_{4k}=r^2\,\mathrm{Im}\,z^k, \quad g_{4k+2}=\mathrm{Re}\,z^{k+2}, \quad g_{4k+3}=\mathrm{Im}\,z^{k+2} \quad k=1,2\cdots \tag{135}$$

In agreement with relations (130), the homogeneous solutions w_i, ψ_{xi}, and ψ_{yi} are obtained in terms of gs and fs as

$$w_i=g-\frac{D}{C}\nabla^2 g, \quad \psi_{xi}=g_{,x}+f_{,y}, \quad \psi_{yi}=g_{,y}-f_{,x} \tag{136}$$

However, since the sets of functions f_k (134) and functions g_j (135) are independent of each other, the submatrices $\mathbf{N}_i=\{w_i,\psi_{xi},\psi_{yi}\}^T$ in Eq. (9) will be of the following two types:

$$\mathbf{N}_i=\begin{Bmatrix} g_j-\dfrac{D}{C}\nabla^2 g_j \\ g_{j,x} \\ g_{j,y}\end{Bmatrix} \tag{137}$$

or

$$\mathbf{N}_i=\begin{Bmatrix} 0 \\ f_{k,y} \\ -f_{k,x}\end{Bmatrix} \tag{138}$$

One of the possible methods of relating index i to corresponding j or k values in Eq. (137) or (138) is displayed in Table 1. However, many other possibilities exist [36]. It should also be pointed out that successful h-method elements have been obtained by Jirousek et al. [34] and Petrolito [37] with only polynomial set of homogeneous solutions. The effect of various loads can accurately be accounted for by a particular solution of the form

$$\breve{\mathbf{u}}=\begin{Bmatrix} \breve{w} \\ \breve{\psi}_x \\ \breve{\psi}_y\end{Bmatrix}=\begin{Bmatrix} \breve{g}-\dfrac{D}{C}\nabla^2\breve{g} \\ \breve{g}_{,x} \\ \breve{g}_{,y}\end{Bmatrix} \tag{139}$$

where $\breve{g}$ is a particular solution of Eq. (132). The most useful solutions are

$$\breve{g}=\frac{\bar{q}r^4}{64D}, \tag{140}$$

for a uniform load $\bar{q}$=constant, and

$$\breve{g} = \frac{\bar{P} r_{PQ}^2}{8\pi D} \ln r_{PQ}, \tag{141}$$

for a concentrated load $\bar{P}$, where r_{PQ} is defined in Sec. 3. A number of particular solutions for Reissner-Mindlin plates can be found in standard texts (e.g., Reismann [144]).

Since evaluation of the element matrices calls for boundary integration only (see Sec. 3, for example), explicit knowledge of the domain interpolation of the auxiliary conforming field is not necessary. As a consequence, the boundary distribution of $\tilde{\mathbf{u}} = \tilde{\mathbf{N}}\mathbf{d}$, referred to as "frame function," is all that is needed.

The elements considered in this section are either p type ($M \neq 0$) (Fig. 1) or conventional type ($M=0$), with three standard degrees of freedom at corner nodes, e.g.,

$$\mathbf{d}_A = \tilde{\mathbf{u}}_A = \{\tilde{w}_A, \tilde{\psi}_{xA}, \tilde{\psi}_{yA}\}^T, \quad \mathbf{d}_B = \tilde{\mathbf{u}}_B = \{\tilde{w}_B, \tilde{\psi}_{xB}, \tilde{\psi}_{yB}\}^T \tag{142}$$

and an optional number M of hierarchical degrees of freedom associated with midside nodes

$$\mathbf{d}_C = \Delta\tilde{\mathbf{u}}_C = \{\Delta\tilde{w}_{C1}, \Delta\tilde{\psi}_{xC1}, \Delta\tilde{\psi}_{yC1}, \Delta\tilde{w}_{C2}, \Delta\tilde{\psi}_{xC2}, \Delta\tilde{\psi}_{yC2}, \cdots \text{etc}.\}^T \tag{143}$$

Within the thin limit $\tilde{\psi}_x = \partial\tilde{w}/\partial x$ and $\tilde{w}_y = \partial\tilde{w}/\partial y$, the order of the polynomial interpolation of $\tilde{w}$ has to be one degree higher than that of ψ_x and ψ_y if the resulting element is to be free of shear locking. Hence, if along a particular side A-C-B of the element (Fig. 1)

$$\tilde{\psi}_{xA\text{-}C\text{-}B} = \tilde{N}_A \tilde{\psi}_{xA} + \tilde{N}_B \tilde{\psi}_{xB} + \sum_{i=1}^{\tilde{p}-1} \tilde{N}_{Ci} \Delta\tilde{\psi}_{xCi} \tag{144}$$

$$\tilde{\psi}_{yA\text{-}C\text{-}B} = \tilde{N}_A \tilde{\psi}_{yA} + \tilde{N}_B \tilde{\psi}_{yB} + \sum_{i=1}^{\tilde{p}-1} \tilde{N}_{Ci} \Delta\tilde{\psi}_{yCi} \tag{145}$$

where $\tilde{N}_A$, $\tilde{N}_B$, and $\tilde{N}_{Ci}$ are defined in Fig. 1, $\tilde{p}$ is the polynomial degree of $\tilde{\psi}_x$ and $\tilde{\psi}_y$ (the last term in Eqs. (144) and (145) will be missing if $\tilde{p}=1$), then the proper choice for the deflection interpolation is

$$\tilde{w}_{A\text{-}C\text{-}B} = \tilde{N}_A \tilde{w}_A + \tilde{N}_B \tilde{w}_B + \sum_{i=1}^{\tilde{p}} \tilde{N}_{Ci} \Delta\tilde{w}_{Ci} \tag{146}$$

The application of these functions for $\tilde{p}=1$ and $\tilde{p}=2$ along with 13 or 25 polynomial homogeneous solutions (137) leads to elements identical to Petrolito's quadrilaterals Q21-13 and Q32-25 [37].

An alternative variational functional presented by Qin [36] for deriving HT thick-plate elements is as follows:

$$\Pi_m = \sum_e \left\{ \Pi_e + \int_{\Gamma_{e2}} (\bar{Q}_n - Q_n)\tilde{w} ds + \int_{\Gamma_{e4}} (\bar{M}_n - M_n)\tilde{\psi}_n ds + \int_{\Gamma_{e6}} (\bar{M}_{ns} - M_{ns})\tilde{\psi}_s ds - \int_{\Gamma_{e7}} (M_n \tilde{\psi}_n + M_{ns}\tilde{\psi}_s + Q_n \tilde{w}) ds \right\} \tag{147}$$

where

$$\Pi_e = \int_{\Omega_e} U d\Omega - \int_{\Gamma_{e1}} \tilde{Q}_n \bar{w} ds - \int_{\Gamma_{e3}} \tilde{M}_n \bar{\psi}_n ds - \int_{\Gamma_{e5}} \tilde{M}_{ns} \bar{\psi}_s ds \tag{148}$$

with

$$U = \frac{1}{2D(1-\mu^2)}[(M_{11}+M_{22})^2 + 2(1+\mu)(M_{12}^2 - M_{11}M_{22})] + \frac{1}{2C}(Q_x^2 + Q_y^2) \tag{149}$$

and where Eqs. (126)–(128) are assumed to be satisfied a priori. The boundary Γ_e of a particular element consists of the following parts:

$$\Gamma_e = \Gamma_{e1} + \Gamma_{e2} + \Gamma_{e7} = \Gamma_{e3} + \Gamma_{e4} + \Gamma_{e7} = \Gamma_{e5} + \Gamma_{e6} + \Gamma_{e7} \tag{150}$$

where

$$\Gamma_{e1} = \Gamma_e \cap \Gamma_w, \quad \Gamma_{e2} = \Gamma_e \cap \Gamma_Q, \quad \Gamma_{e3} = \Gamma_e \cap \Gamma_{\psi_n}, \quad \Gamma_{e4} = \Gamma_e \cap \Gamma_{M_n}$$

$$\Gamma_{e5} = \Gamma_e \cap \Gamma_{\psi_s}, \quad \Gamma_{e6} = \Gamma_e \cap \Gamma_{M_{ns}} \tag{151}$$

and Γ_{e7} is the interelement boundary of the element.

The extension to thick plates on an elastic foundation is similar to that in Sec. 5. In the case of a thick plate resting on an elastic foundation, the left-hand side of Eq. (128) and the boundary equation (122) must be augmented by the terms Kw and $-\alpha G_p w$, respectively,

$$C\left(\nabla^2 w - \frac{\partial\psi_x}{\partial x} - \frac{\partial\psi_y}{\partial y}\right) + Kw = \bar{q} \quad (\text{in } \Omega) \tag{152}$$

$$M_n = M_{ij}n_i n_j - \alpha G_p w = \bar{M}_n \quad (\text{on } \Gamma_{Mn}) \tag{153}$$

where α and K are as defined in Sec. 5.

As discussed before, the transverse deflection w and the rotations ψ_x, ψ_y may be expressed in terms of two auxiliary functions, g and f, by the first part of Eq. (136) and Eq. (130). The function f is again obtained as a solution of the modified Bessel equation (second part of Eq. (132)), while for g, instead of the biharmonic equation (first part of Eq. (132)), the following differential equation now applies [36]:

$$D\nabla^4 g + \frac{K}{C}\nabla^2 g - Kg = \bar{q} \tag{154}$$

The corresponding T-complete system of homogeneous solutions is obtained in a manner similar to that in Sec. 5, as

$$g(r,\theta) = c_1 G_0(r) + \sum_{j=1}^{\infty} [c_{2j} G_j(r)\cos j\theta + c_{2j+1} G_j(r)\sin j\theta] \tag{155}$$

where

$$G_j(r) = I_j(r\sqrt{C_2}) - J_j(r\sqrt{C_1}) \tag{156}$$

with

$$C_1 = \sqrt{\left(\frac{k_w}{2C}\right)^2 + \frac{k_w}{D}} + \frac{k_w}{2C}, \quad C_2 = \sqrt{\left(\frac{k_w}{2C}\right)^2 + \frac{k_w}{D}} - \frac{k_w}{2C} \tag{157}$$

for a Winkler-type foundation and

$$C_1 = \frac{\sqrt{b} + k_P/C + G_P/D}{2(1 - G_P/C)}, \quad C_2 = \frac{\sqrt{b} - k_P/C - G_P/D}{2(1 - G_P/C)} \tag{158}$$

$$b = \left(\frac{k_P}{C} + \frac{G_P}{D}\right)^2 + \frac{4k_P}{D}\left(1 - \frac{G_p}{C}\right) \tag{159}$$

for a Pasternak-type foundation.

The variational functional used to derive HT FE formulation for thick plates on an elastic foundation is the same as Eq. (147) except that the strain energy function U in Eq. (149) is now replaced by U^*

$$U^* = U + V^*, \tag{160}$$

in which U and V^* are defined in Eqs. (149) and (114), respectively.

7 Transient Heat Conduction

Consider a two-dimensional heat conduction equation that describes the unsteady temperature distribution in a solid (domain Ω). This problem is governed by the differential equation

$$k\nabla^2 u + \bar{Q} = \rho c \frac{\partial u}{\partial t}, \tag{161}$$

subject to the initial condition in $\bar{\Omega}$

$$u(x,y,0) = u_0(x,y) \tag{162}$$

and the boundary conditions on Γ

$$u(x,y,t) = \bar{u}(x,y,t) \quad (\text{on } \Gamma_1) \tag{163}$$

$$p(x,y,t) = \bar{p}(x,y,t) \quad (\text{on } \Gamma_2) \tag{164}$$

$$q(x,y,t) = \bar{q}(x,y,t) \quad (\text{on } \Gamma_3) \tag{165}$$

in which

$$p = k\frac{\partial u}{\partial n}, \quad q = hu + p, \quad \bar{q} = hu_{\text{env}} \tag{166}$$

$$\bar{\Omega} = \Omega + \Gamma, \quad \Gamma = \Gamma_1 + \Gamma_2 + \Gamma_3 \tag{167}$$

where $u(x,y,t)$ is the temperature function, $\bar{Q}$ the body heat source, k the specified thermal conductivity, ρ the density, and c the specific heat. Furthermore, u_0 is the initial temperature, h is the heat transfer coefficient, and u_{env} stands for environmental temperature.

The initial boundary value problem (161)–(165) cannot, in general, be solved analytically. Hence, the time domain is divided into N equal intervals and denoted $\Delta t = t_m - t_{m-1}$. Consider now a typical time interval $[t_m, t_{m+1}]$, in which u and $\bar{Q}$ are approximated by a linear function

$$u(t) \approx \frac{1}{\Delta t}[(t - t_m)u_{m+1} - (t - t_{m+1})u_m] \tag{168}$$

$$\bar{Q}(t) \approx \frac{1}{\Delta t}[(t - t_m)\bar{Q}_{m+1} - (t - t_{m+1})\bar{Q}_m] \tag{169}$$

The integral of Eq. (161) over the time interval $[t_m, t_{m+1}]$ yields

$$u_{m+1} = u_m + \frac{\Delta t}{2\rho c}[k\nabla^2 u_m + k\nabla^2 u_{m+1} + \bar{Q}_m + \bar{Q}_{m+1}] \tag{170}$$

From this we arrive at the following single time-step formula [48]:

$$(\nabla^2 - a^2)u_m = b_m \tag{171}$$

with the boundary conditions

$$u_m = \bar{u}_m \ (\text{on } \Gamma_1), \quad p_m = \bar{p}_m \ (\text{on } \Gamma_2), \quad q_m = \bar{q}_m \ (\text{on } \Gamma_3) \tag{172}$$

where

$$p_m = k\frac{\partial u_m}{\partial n}, \quad q_m = hu_m + p_m \tag{173}$$

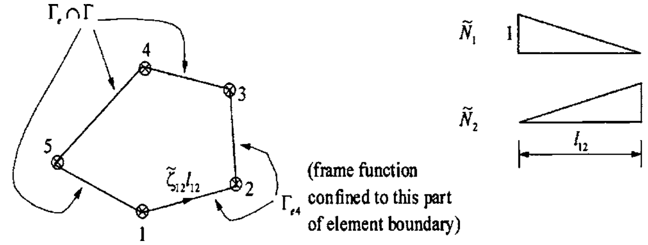

Fig. 7 A typical HT element with linear frame function

$$a^2 = \frac{2\rho c}{k\Delta t}, \quad b_m = -(\nabla^2 + a^2)u_{m-1} - \frac{1}{k}(\bar{Q}_m + \bar{Q}_{m-1}) \tag{174}$$

and where $\bar{u}_m$, $\bar{p}_m$, and $\bar{q}_m$ stand for imposed quantities at the time $t = t_m$. Hereafter, to further simplify the writing, we shall omit the index m appearing in Eqs. (171) and (172).

Consider again the boundary value problem defined in Eqs. (171)–(174). The domain is subdivided into elements and over each element e the assumed field is defined in Eq. (9), where $\breve{u}$ and N_j are known functions, which satisfy

$$(\nabla^2 - a^2)\breve{u} = b, \quad (\nabla^2 - a^2)N_j = 0 \quad (\text{on } \Omega_e) \tag{175}$$

The second equation of (175) is the modified Bessel equation, for which a T-complete system of homogeneous solution can be expressed, in polar coordinates r and θ, as

$$N_{2m} = I_m(ar)\sin m\theta, \quad N_{2m+1} = I_m(ar)\cos m\theta \quad (m = 0,1,2,\cdots) \tag{176}$$

The particular solution $\breve{u}$ of Eq. (175) for any right-hand side b can be obtained by integration of the source function

$$u^*(r_{PQ}) = \frac{1}{2\pi}K_0(ar_{PQ}) \tag{177}$$

As a consequence, the particular solution $\breve{u}$ of Eq. (171) can be expressed as

$$\breve{u}(P) = \frac{1}{2\pi}\int_{\Omega_e} b(Q)K_0(ar_{PQ})d\Omega(Q) \tag{178}$$

The area integration in Eq. (178) can be performed by numerical quadrature using the Gauss-Legendre rule.

The auxiliary interelement frame field $\tilde{u}$ used here is confined to the interelement portion of the element boundary Γ_e

$$\Gamma_e = \Gamma_{e1} + \Gamma_{e2} + \Gamma_{e4} + \Gamma_{e4} \tag{179}$$

where

$$\Gamma_{e1} = \Gamma_e \cap \Gamma_1, \quad \Gamma_{e2} = \Gamma_e \cap \Gamma_2, \quad \Gamma_{e3} = \Gamma_e \cap \Gamma_3 \tag{180}$$

and where Γ_{e4} is the interelement portion of Γ_e (see Fig. 7), as opposed to standard HT elements discussed previously (where $\tilde{u}$ extends over the whole element boundary Γ_e). The obvious advantage of such a formulation is the decrease in the number of degrees of freedom for the element assembly. In our case, we assume

$$\tilde{u} = \tilde{\mathbf{N}}\mathbf{d} \quad (\text{on } \Gamma_{e4}) \tag{181}$$

As an example, Fig. 7 displays a typical HT element with an arbitrary number of sides. In the simplest case, with linear shape function, the vector of nodal parameters is defined as

$$\mathbf{d} = \{\tilde{u}_1, \tilde{u}_2, \tilde{u}_3\}^T \tag{182}$$

and along a particular element side situated on Γ_{4e}, for example, the side 1-2, we have simply

$$\tilde{u} = \tilde{N}_1 \tilde{u}_1 + \tilde{N}_2 \tilde{u}_2 \tag{183}$$

where

$$\tilde{N}_1 = 1 - \tilde{\zeta}_{12}, \quad \tilde{N}_2 = \tilde{\zeta}_{12} \tag{184}$$

There are no degrees of freedom at nodes 4 and 5 situated on $\Gamma_e \cap \Gamma$ (Γ is the boundary of the domain).

To enforce the boundary conditions (172) and the interelement continuity on u, we minimize for each element the following least-squares functional

$$\int_{\Gamma_{e1}} (u-\bar{u})^2 ds + d^2 \int_{\Gamma_{e2}} (p-\bar{p})^2 ds + d^2 \int_{\Gamma_{e3}} (q-\bar{q})^2 ds + \int_{\Gamma_{e4}} (u-\tilde{u})^2 ds = \min \tag{185}$$

where $d > 0$ is an arbitrary chosen length (in this section d is chosen as the average distance between the element center and element corners defined in Eq. (3.51) of Qin [61]), which serves the purpose of obtaining a physically meaningful functional (homogeneity of physical units). The least-squares statement (185) yields for the internal parameter $\mathbf{c}$ the following system of linear equations:

$$\mathbf{Ac} = \mathbf{a} + \mathbf{Wd} \tag{186}$$

where

$$\mathbf{A} = \int_{\Gamma_{e1} \cup \Gamma_{e4}} \mathbf{N}^T \mathbf{N} ds + d^2 \int_{\Gamma_{e2}} \mathbf{P}^T \mathbf{P} ds + d^2 \int_{\Gamma_{e3}} \mathbf{Q}^T \mathbf{Q} ds \tag{187}$$

$$\mathbf{a} = \int_{\Gamma_{e1}} \mathbf{N}^T (\bar{u} - \breve{u}) ds + d^2 \int_{\Gamma_{e2}} \mathbf{P}^T (\bar{p} - \breve{p}) ds + d^2 \int_{\Gamma_{e3}} \mathbf{Q}^T (\bar{q} - \breve{q}) ds \tag{188}$$

$$\mathbf{W} = \int_{\Gamma_{e4}} \mathbf{N}^T \tilde{\mathbf{N}} ds \tag{189}$$

From Eqs. (186)–(189), the internal coefficients $\mathbf{c}$ are readily expressed in terms of the nodal parameters $\mathbf{d}$

$$\mathbf{c} = \breve{\mathbf{c}} + \mathbf{Cd} \tag{190}$$

where

$$\breve{\mathbf{c}} = \mathbf{A}^{-1} \mathbf{a}, \quad \mathbf{C} = \mathbf{A}^{-1} \mathbf{W} \tag{191}$$

We now address evaluation of the element matrices. In order to enforce "traction reciprocity"

$$\frac{\partial u_e}{\partial n_e} + \frac{\partial u_f}{\partial n_f} = 0, \quad (\text{on } \Gamma_e \cup \Gamma_f) \tag{192}$$

and to obtain a symmetric positive definite stiffness matrix, we set, in a similar way as in [63],

$$k \int_{\Gamma_e} \frac{\partial u}{\partial n} \delta u ds = \int_{\Gamma_{e2}} \bar{p} \delta u ds + \int_{\Gamma_{e3}} \bar{q} \delta u ds - h \int_{\Gamma_{e4}} u \delta u ds + k \delta \mathbf{d}^T \mathbf{r} \tag{193}$$

where $\mathbf{r}$ stands for the vector of fictitious equivalent nodal forces conjugate to the nodal displacement $\mathbf{d}$. This leads to the customary "force-displacement" relationship

$$\mathbf{r} = \breve{\mathbf{r}} + \mathbf{kd} \tag{194}$$

where

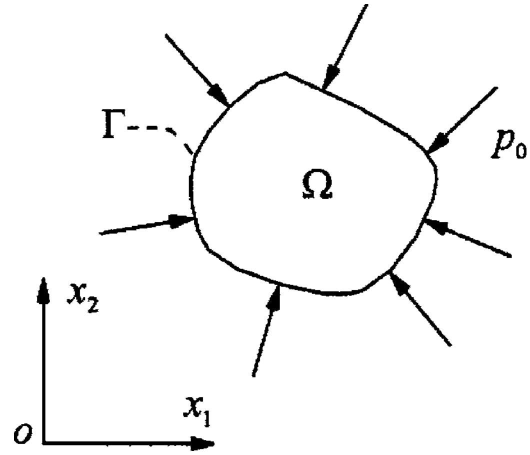

Fig. 8 Geometry and loading condition of the thin plate

$$\breve{\mathbf{r}} = \mathbf{C}^T (\mathbf{H} \breve{\mathbf{c}} + \mathbf{h}) \quad \text{and} \quad \mathbf{k} = \mathbf{C}^T \mathbf{HC} \tag{195}$$

The auxiliary matrices $\mathbf{h}$ and $\mathbf{H}$ are calculated by setting

$$\frac{\partial u}{\partial n} = \frac{\partial}{\partial n} (\breve{u} + \mathbf{Nc}) = \breve{t} + \mathbf{Tc} \tag{196}$$

and then performing the following boundary integrals:

$$\mathbf{h} = \int_{\Gamma_e} \mathbf{N}^T \breve{t} ds - \frac{1}{k} \left\{ \int_{\Gamma_{e2}} \mathbf{N}^T \bar{p} ds + \int_{\Gamma_{e3}} \mathbf{N}^T (\bar{s} - h \breve{u}) ds \right\} \tag{197}$$

$$\mathbf{H} = \int_{\Gamma_e} \mathbf{N}^T \mathbf{T} ds + \frac{h}{k} \int_{\Gamma_{e3}} \mathbf{N}^T \mathbf{N} ds \tag{198}$$

Through integration by parts, it is easy to show that the first integral in Eq. (198) may be written as

$$\int_{\Gamma_e} \mathbf{N}^T \mathbf{T} ds = \int_{\Gamma_e} \mathbf{B}^T \mathbf{B} ds \tag{199}$$

where

$$\mathbf{B} = \left\{ \frac{\partial \mathbf{N}}{\partial x}, \frac{\partial \mathbf{N}}{\partial y} \right\}^T \tag{200}$$

As a consequence, $\mathbf{H}$ is a symmetric matrix.

8 Postbuckling Bending of Thin Plate

In this section, the application of HT elements to postbuckling of thin-plate bending problems is reviewed. The thin plate system is subjected to in-plane pressure with or without elastic foundation.

Let us consider a thin isotropic plate of uniform thickness t, occupying a two-dimensional arbitrarily shaped region Ω bounded by its boundary Γ (Fig. 8). The plate is subjected to an external radial uniform in-plane compressive load p_0 (per unit length at the boundary Γ). The field equations governing the postbuckling behavior of thin plate has been detailed in [145,146].

In this application the internal fields have two parts. One is the in-plane field $\mathbf{u}_{\text{in}} (=\{u_1, u_2\}^T)$ and the other is the out-of-plane field $\mathbf{u}_{\text{out}} (=w)$. They are identified by subscripts "in" and "out" respectively, and are assumed as follows:

$$\mathbf{u}_{\text{in}} = \begin{Bmatrix} \dot{u}_1 \\ \dot{u}_2 \end{Bmatrix} = \breve{\mathbf{u}}_{\text{in}} + \begin{Bmatrix} \mathbf{N}_1 \\ \mathbf{N}_2 \end{Bmatrix} \mathbf{c}_{\text{in}} = \breve{\mathbf{u}}_{\text{in}} + \mathbf{N}_{\text{in}} \mathbf{c}_{\text{in}} \tag{201}$$

$$\mathbf{u}_{\text{out}} = \dot{w} = \breve{w} + \mathbf{N}_3\mathbf{c}_{\text{out}} \tag{202}$$

where $\mathbf{c}_{\text{in}}$ and $\mathbf{c}_{\text{out}}$ are two undetermined coefficient vectors and $\breve{\mathbf{u}}_{\text{in}}$, $\breve{w}$, $\mathbf{N}_{\text{in}}$, and $\mathbf{N}_3$ are known functions, which satisfy

$$\begin{bmatrix} L_1 & L_2 \\ L_2 & L_3 \end{bmatrix}\breve{\mathbf{u}}_{\text{in}} = \begin{Bmatrix} \dot{P}_1 \\ \dot{P}_2 \end{Bmatrix}, \quad \begin{bmatrix} L_1 & L_2 \\ L_2 & L_3 \end{bmatrix}\begin{Bmatrix} \mathbf{N}_1 \\ \mathbf{N}_2 \end{Bmatrix} = 0 \quad (\text{in } \Omega_e) \tag{203a}$$

$$L_4\breve{w} = \dot{P}_3, \quad L_4\mathbf{N}_3 = 0 \quad (\text{in } \Omega_e) \tag{203b}$$

and where L_i have been defined in [49,61], $\mathbf{N}_{\text{in}}$ and $\mathbf{N}_3$ are formed by suitably truncated T-complete systems of the governing equation [61]:

$$L_1\dot{u}_1 + L_2\dot{u}_2 = \dot{P}_1$$

$$L_2\dot{u}_1 + L_3\dot{u}_2 = \dot{P}_2$$

$$L_4\dot{w} = \dot{P}_3 \tag{204}$$

The T-complete functions corresponding to the first two lines of Eq. (204) have been given in expressions (80)–(83), while the Trefftz functions related to the third line of Eq. (204) are [61]

$$T = \{f_0(r), f_m(r)\cos m\theta, f_m(r)\sin m\theta\} = \{T_i\} \tag{205}$$

where $f_m(r) = r^m - J_m(\lambda r)$.

All that is left is to determine the parameters $\mathbf{c}$ so as to enforce on $\mathbf{u}(=\{\dot{u}_1, \dot{u}_2, \dot{w}\}^T)$ interelement conformity ($\mathbf{u}_e = \mathbf{u}_f$ on $\Gamma_e \cap \Gamma_f$) and the related boundary conditions, where e and f stand for any two neighbouring elements. This can be completed by linking the Trefftz-type solutions (201) and (202) through an interface displacement frame surrounding the element, which is approximated in terms of the same degrees of freedom, $\mathbf{d}$, as used in the conventional elements

$$\tilde{\mathbf{u}} = \tilde{\mathbf{N}}\mathbf{d} \tag{206}$$

where

$$\tilde{\mathbf{u}} = \{\tilde{\mathbf{u}}_{\text{in}}, \tilde{\mathbf{u}}_{\text{out}}\}^T \tag{207}$$

$$\tilde{\mathbf{u}}_{\text{in}} = \{\tilde{u}_1, \tilde{u}_2\}^T = \begin{bmatrix} \tilde{\mathbf{N}}_1 \\ \tilde{\mathbf{N}}_2 \end{bmatrix}\mathbf{d}_{\text{in}} = \tilde{\mathbf{N}}_{\text{in}}\mathbf{d}_{\text{in}} \tag{208}$$

$$\tilde{\mathbf{u}}_{\text{out}} = \{\tilde{w}, \tilde{w}_{,n}\}^T = \begin{bmatrix} \tilde{\mathbf{N}}_3 \\ \tilde{\mathbf{N}}_4 \end{bmatrix}\mathbf{d}_{\text{out}} = \tilde{\mathbf{N}}_{\text{out}}\mathbf{d}_{\text{out}} \tag{209}$$

$$\mathbf{d} = \{\mathbf{d}_{\text{in}}, \mathbf{d}_{\text{out}}\}^T \tag{210}$$

and where $\mathbf{d}_{\text{in}}$ and $\mathbf{d}_{\text{out}}$ stand for nodal parameter vectors of the in-plane and out-of-plane displacements, and $\tilde{\mathbf{N}}_i = (i=1\text{–}4)$ are the conventional FE interpolation functions.

The particular solutions $\breve{\mathbf{u}}_{\text{in}}$ and $\breve{w}$ in Eq. (201) and (202) are obtained by means of a source-function approach. The source functions corresponding to Eq. (204) can be found in [146]

$$u_{ij}^*(r_{PQ}) = \frac{1+\mu}{4\pi E}[-(3-\mu)\delta_{ij}\ln r_{PQ} + (1+\mu)r_{PQ,i}r_{PQ,j}] \tag{211}$$

$$w^*(r_{PQ}) = \frac{1}{4\pi D\lambda^2}[2\ln r_{PQ} - \pi Y_0(\lambda r_{PQ})] \tag{212}$$

where $u_{ij}^*(r_{PQ})$ represents the ith component of in-plane displacement at the field point P of an infinite plate when a unit point force ($j=1,2$) is applied at the source point Q, while $w^*(r_{PQ})$ stands for the deflection at point P due to a unit transverse force applied at point Q. Using these source functions, the particular solutions $\breve{\mathbf{u}}_{\text{in}}$ and $\breve{w}$ can be expressed as

$$\breve{\mathbf{u}}_{\text{in}} = \int_\Omega \dot{P}_j \begin{Bmatrix} u_{1j}^* \\ u_{2j}^* \end{Bmatrix} d\Omega \tag{213}$$

$$\breve{w} = \int_\Omega \dot{P}_3 w^* d\Omega \tag{214}$$

The element matrix equation can be generated by way of following functionals [61]:

$$\begin{aligned}\Pi_{me(\text{in})} = {}& \frac{1}{2}\int_{\Omega_e} \dot{P}_i\dot{u}_i d\Omega - \int_{\Gamma_{e1}} \dot{\bar{N}}_n \dot{\tilde{u}}_n ds - \int_{\Gamma_{e3}} \dot{\bar{N}}_{ns}\dot{\tilde{u}}_s ds \\ & - \int_{\Gamma_{e2}} (\dot{N}_n - \bar{N}_n^*)\dot{\tilde{u}}_n ds - \int_{\Gamma_{e4}} (\dot{N}_{ns} - \bar{N}_{ns}^*)\dot{\tilde{u}}_s ds \\ & + \frac{1}{2}\int_{\Gamma_e} \mathbf{t}_{\text{in}}\mathbf{u}_{\text{in}} ds - \int_{\Gamma_{e9}} \mathbf{t}_{\text{in}}\tilde{\mathbf{u}}_{\text{in}} ds\end{aligned} \tag{215}$$

$$\begin{aligned}\Pi_{me(\text{out})} = {}& \frac{1}{2}\int_{\Omega_e} \dot{P}_3\dot{w} d\Omega + \int_{\Gamma_{e5}} \dot{\bar{M}}_n \dot{\tilde{w}}_{,n} ds - \int_{\Gamma_{e7}} \dot{\bar{R}}\dot{\tilde{w}} ds \\ & + \int_{\Gamma_{e6}} (\dot{M}_n - \dot{\bar{M}}_n)\dot{\tilde{w}}_{,n} ds - \int_{\Gamma_{e8}} (\dot{R} - \bar{R}^*)\dot{\tilde{w}} ds \\ & + \frac{1}{2}\int_{\Gamma_e} \mathbf{t}_{\text{out}}\mathbf{u}_{\text{out}} ds - \int_{\Gamma_{e9}} \mathbf{t}_{\text{out}}\tilde{\mathbf{u}}_{\text{out}} ds.\end{aligned} \tag{216}$$

The boundary Γ_e of a particular element here consists of the following parts:

$$\begin{aligned}\Gamma_e &= \Gamma_{e1} + \Gamma_{e2} + \Gamma_{e9} = \Gamma_{e3} + \Gamma_{e4} + \Gamma_{e9} = \Gamma_{e5} + \Gamma_{e6} + \Gamma_{e9} \\ &= \Gamma_{e7} + \Gamma_{e8} + \Gamma_{e9}\end{aligned} \tag{217}$$

where

$$\Gamma_{e1} = \Gamma_e \cap \Gamma_{u_n}, \quad \Gamma_{e2} = \Gamma_e \cap \Gamma_{N_n}, \quad \Gamma_{e3} = \Gamma_e \cap \Gamma_{u_s}$$

$$\Gamma_{e4} = \Gamma_e \cap \Gamma_{N_{ns}}, \quad \Gamma_{e5} = \Gamma_e \cap \Gamma_{w_n}, \quad \Gamma_{e6} = \Gamma_e \cap \Gamma_{M_n}$$

$$\Gamma_{e7} = \Gamma_e \cap \Gamma_w, \quad \Gamma_{e8} = \Gamma_e \cap \Gamma_R \tag{218}$$

and Γ_{e9} represents the interelement boundary of the element.

Extension to postbuckling plate on an elastic foundation is similar to the treatment in Sec. 5. In this case the left-hand side of the third line of Eq. (204) and the boundary equation $\dot{M}_n = \dot{M}_{ij}n_in_j = \dot{\bar{M}}_n$ must be augmented by the terms $K\dot{w}$ and $\alpha G_P\dot{w}$, respectively,

$$L_4\dot{w} + K\dot{w} = \dot{P}_3 \tag{219}$$

$$\dot{M}_n = \dot{M}_{ij}n_in_j - \alpha G_P\dot{w} = \dot{\bar{M}}_n \tag{220}$$

where α, K, and G_P are defined in Sec. 5.

The Trefftz functions of Eq. (219) can be obtained by considering the corresponding homogeneous equation

$$(L_4+K)g=(\nabla^4+\eta^2\nabla^2+S)g=(\nabla^2+b_1)(\nabla^2+b_2)g=0 \tag{221}$$

As a consequence, the T-complete system of Eq. (221) is obtained as [61]

$$\mathrm{T}=\{f_0(r), f_m(r)\sin m\theta, f_m(r)\cos m\theta\}=\{T_i\} \tag{222}$$

where $f_m(r)=J_m(r\sqrt{b_1})-J_m(r\sqrt{b_2})$, with $b_{1,2}=\lambda^2 \mp \sqrt{\lambda^4-4k_w/D}$ for a Winkler-type foundation.

9 Geometrically Nonlinear Analyses of Thick Plates

Employment of Trefftz-element approach enabled Qin [50] and Qin and Diao [52] to solve for the first time a large deflection problem of thick plate with or without elastic foundation. Formulations presented in this section are based on the developments mentioned above.

Consider a Mindlin-Reissner plate of uniform thickness t, occupying a two-dimensional arbitrarily shaped region Ω with boundary Γ. The nonlinear behavior of the plate for moderately large deflection is governed by the following incremental equations [147]:

$$L_1\dot{u}_1+L_2\dot{u}_2=\dot{P}_1 \tag{223}$$

$$L_2\dot{u}_1+L_3\dot{u}_2=\dot{P}_2 \tag{224}$$

$$L_{33}\dot{w}+L_{34}\dot{\psi}_1+L_{35}\dot{\psi}_2=\dot{P}_3+\dot{q} \tag{225}$$

$$L_{43}\dot{w}+L_{44}\dot{\psi}_1+L_{45}\dot{\psi}_2=0 \tag{226}$$

$$L_{53}\dot{w}+L_{54}\dot{\psi}_1+L_{55}\dot{\psi}_2=0 \tag{227}$$

together with

$$\dot{u}_n=\dot{u}_i n_i=\dot{\bar{u}}_n \ (\text{on } \Gamma_{u_n}), \quad \dot{u}_s=\dot{u}_i s_i=\dot{\bar{u}}_s \ (\text{on } \Gamma_{u_s}) \tag{228}$$

$$\dot{N}_n=\dot{N}^l_{ij}n_i n_j=\dot{\bar{N}}_n-\dot{N}^n_{ij}n_i n_j=\bar{N}^*_n \quad (\text{on } \Gamma_{N_n}) \tag{229}$$

$$\dot{N}_{ns}=\dot{N}^l_{ij}n_i s_j=\dot{\bar{N}}_{ns}-\dot{N}^n_{ij}n_i s_j=\bar{N}^*_{ns} \quad (\text{on } \Gamma_{N_{ns}}) \tag{230}$$

for in-plane boundary condition and

$$\dot{w}=\dot{\bar{w}} \ (\text{on } \Gamma_w), \quad \dot{\psi}_n=\dot{\psi}_i n_i=\dot{\bar{\psi}}_n \ (\text{on } \Gamma_{\psi_n}), \quad \dot{\psi}_s=\dot{\psi}_i s_i=\dot{\bar{\psi}}_s \ (\text{on } \Gamma_{\psi_s}) \tag{231}$$

for clamped edge, or

$$\dot{w}=\dot{\bar{w}} \ (\text{on } \Gamma_w), \quad \dot{\psi}_s=\dot{\bar{\psi}}_s \ (\text{on } \Gamma_{\psi_s}), \quad \dot{M}_n=\dot{M}_{ij}n_i n_j=\dot{\bar{M}}_n \ (\text{on } \Gamma_{M_n}) \tag{232}$$

for simply supported edge, or

$$\dot{M}_n=\dot{\bar{M}}_n \ (\text{on } \Gamma_{M_n}), \quad \dot{M}_{ns}=\dot{M}_{ij}n_i s_j=\dot{\bar{M}}_{ns} \ (\text{on } \Gamma_{M_{ns}}),$$
$$\dot{R}=\dot{Q}_i n_i=\dot{\bar{R}}-\dot{R}^n=\bar{R}^* \ (\text{on } \Gamma_R) \tag{233}$$

for free edge, where $R^n=N_n w_{,n}+N_{ns}w_{,s}$, L_1, L_2, L_3, and $\dot{P}_1, \dot{P}_2, \dot{P}_3$ are defined in [61], $\dot{q}$ represents the transverse distributed load, and

$$L_{33}=C\nabla^2, \quad L_{34}()=-L_{43}()=-C()_{,1}, \quad L_{35}=-L_{53}=-C()_{,2}$$
$$L_{44}=DL_1-C, \quad L_{45}=L_{54}=DL_2, \quad L_{55}=DL_3-C \tag{234}$$

As noted before, the HT FE model is based on assuming two sets of distinct displacements, the internal field $\mathbf{u}$ and the frame field $\tilde{\mathbf{u}}$. The internal field $\mathbf{u}$ fulfil's the governing differential equations (223)–(227) identically and is assumed over each element as

$$\mathbf{u}=\begin{Bmatrix}\mathbf{u}_{\text{in}}\\ \mathbf{u}_{\text{out}}\end{Bmatrix}=\begin{Bmatrix}\breve{\mathbf{u}}_{\text{in}}\\ \breve{\mathbf{u}}_{\text{out}}\end{Bmatrix}+\begin{bmatrix}\mathbf{N}_{\text{in}} & 0\\ 0 & \mathbf{N}_{\text{out}}\end{bmatrix}\begin{Bmatrix}\mathbf{c}_{\text{in}}\\ \mathbf{c}_{\text{out}}\end{Bmatrix}=\breve{\mathbf{u}}+\mathbf{Nc} \tag{235}$$

where

$$\mathbf{u}_{\text{in}}=\{\dot{u}_1, \dot{u}_2\}^T, \quad \mathbf{u}_{\text{out}}=\{\dot{w}, \dot{\psi}_1, \dot{\psi}_2\}^T, \quad \breve{\mathbf{u}}_{\text{in}}=\{\breve{u}_1, \breve{u}_2\}^T,$$
$$\breve{\mathbf{u}}_{\text{out}}=\{\breve{w}, \breve{\psi}_1, \breve{\psi}_2\}^T \tag{236}$$

and where $\breve{\mathbf{u}}_{\text{in}}$, $\breve{\mathbf{u}}_{\text{out}}$, $\mathbf{N}_{\text{in}}$, $\mathbf{N}_{\text{out}}$ are known functions, which satisfy

$$\mathbf{L}_{\text{in}}\breve{\mathbf{u}}_{\text{in}}=\begin{Bmatrix}\dot{P}_1\\ \dot{P}_2\end{Bmatrix}, \quad \mathbf{L}_{\text{in}}\mathbf{N}_{\text{in}}=\mathbf{L}_{\text{in}}\begin{Bmatrix}\mathbf{N}_1\\ \mathbf{N}_2\end{Bmatrix}=0 \quad (\text{on } \Omega_e) \tag{237}$$

$$\mathbf{L}_{\text{out}}\breve{\mathbf{u}}_{\text{out}}=\begin{Bmatrix}\dot{P}_3+\dot{q}\\ 0\\ 0\end{Bmatrix}, \quad \mathbf{L}_{\text{out}}\mathbf{N}_{\text{out}}=\mathbf{L}_{\text{out}}\begin{Bmatrix}\mathbf{N}_3\\ \mathbf{N}_4\\ \mathbf{N}_5\end{Bmatrix}=0 \quad (\text{on } \Omega_e) \tag{238}$$

with

$$\mathbf{L}_{\text{in}}=\begin{bmatrix}L_1 & L_2\\ L_2 & L_3\end{bmatrix}, \quad \mathbf{L}_{\text{out}}=\begin{bmatrix}L_{33} & L_{34} & L_{35}\\ L_{43} & L_{44} & L_{45}\\ L_{53} & L_{54} & L_{55}\end{bmatrix} \tag{239}$$

The interpolation functions $\mathbf{N}_{\text{in}}$ and $\mathbf{N}_{\text{out}}$ are formed by suitably truncated complete systems (80)–(83), (134), and (135).

In order to enforce on $\mathbf{u}$ the conformity, $\mathbf{u}_e=\mathbf{u}_f$ on $\Gamma_e \cap \Gamma_f$ (where e and f stand for any two neighboring elements), as was done before, an auxiliary conforming frame field of the form

$$\tilde{\mathbf{u}}=\tilde{\mathbf{N}}\mathbf{d} \tag{240}$$

is defined at the element boundary Γ_e in terms of parameter $\mathbf{d}$, where

$$\tilde{\mathbf{u}}=\begin{Bmatrix}\tilde{\mathbf{u}}_{\text{in}}\\ \tilde{\mathbf{u}}_{\text{out}}\end{Bmatrix}, \quad \mathbf{d}=\begin{Bmatrix}\mathbf{d}_{\text{in}}\\ \mathbf{d}_{\text{out}}\end{Bmatrix} \tag{241}$$

$$\tilde{\mathbf{u}}_{\text{in}}=\begin{Bmatrix}\tilde{u}_1\\ \tilde{u}_2\end{Bmatrix}=\begin{bmatrix}\tilde{\mathbf{N}}_1\\ \tilde{\mathbf{N}}_2\end{bmatrix}\mathbf{d}_{\text{in}}, \quad \tilde{\mathbf{u}}_{\text{out}}=\begin{Bmatrix}\tilde{w}\\ \tilde{\psi}_1\\ \tilde{\psi}_2\end{Bmatrix}=\begin{bmatrix}\tilde{\mathbf{N}}_3\\ \tilde{\mathbf{N}}_4\\ \tilde{\mathbf{N}}_5\end{bmatrix}\mathbf{d}_{\text{out}} \tag{242}$$

and where $\tilde{\mathbf{N}}_i$ ($i=1$–5) are the usual interpolation functions.

The in-plane particular solution $\breve{\mathbf{u}}_{\text{in}}$ can be calculated through use of Eqs. (211) and (213), whereas the source functions used for calculating the particular solutions of deflection and rotations $\breve{\mathbf{u}}_{\text{out}}$ are now as follows [147]:

$$w^*(r_{PQ})=-\frac{1}{2\pi D\lambda^2}\left[\frac{2}{1-\mu}\ln(\lambda r_{PQ})-\frac{\lambda^2 r_{PQ}^2}{4}[\ln(\lambda r_{PQ})-1]\right] \tag{243}$$

$$\psi_1^*(r_{PQ})=-\frac{r_{PQ}r_{PQ,1}}{4\pi D}[\ln(\lambda r_{PQ})-1/2] \tag{244}$$

$$\psi_2^*(r_{PQ}) = -\frac{r_{PQ} r_{PQ,2}}{4\pi D}[\ln(\lambda r_{PQ}) - 1/2] \tag{245}$$

where $\lambda^2 = 10(1-\mu)/t^2$. Hence, the particular solution $\breve{\mathbf{u}}_{\text{out}}$ is given by

$$\breve{\mathbf{u}}_{\text{out}} = \begin{Bmatrix} \breve{w} \\ \breve{\psi}_1 \\ \breve{\psi}_2 \end{Bmatrix} = \int_{\Omega_e} (\dot{P}_3 + \dot{q}) \begin{Bmatrix} w^* \\ \psi_1^* \\ \psi_2^* \end{Bmatrix} d\Omega \tag{246}$$

The functionals used for deriving the HT FE formulation of nonlinear thick plates can be constructed as [61]:

$$\begin{aligned} \Pi_{me\ (\text{in})} = & \frac{1}{2}\int_{\Omega_e} \dot{P}_i \dot{u}_i d\Omega - \int_{\Gamma_{e1}} \dot{N}_n \dot{\bar{u}}_n ds - \int_{\Gamma_{e3}} \dot{N}_{ns} \dot{\bar{u}}_s ds \\ & - \int_{\Gamma_{e2}} (\dot{N}_n - \bar{N}_n^*) \dot{u}_n ds - \int_{\Gamma_{e4}} (\dot{N}_{ns} - \bar{N}_{ns}^*) \dot{u}_s ds \\ & + \frac{1}{2}\int_{\Gamma_e} \mathbf{t}_{\text{in}} \mathbf{u}_{\text{in}} ds - \int_{\Gamma_{e11}} \mathbf{t}_{\text{in}} \tilde{\mathbf{u}}_{\text{in}} ds \end{aligned} \tag{247}$$

$$\begin{aligned} \Pi_{me\ (\text{out})} = & \frac{1}{2}\int_{\Omega_e} (\dot{P}_3 + \dot{q}) \dot{w} d\Omega - \int_{\Gamma_{e5}} \dot{R} \dot{\bar{w}} ds - \int_{\Gamma_{e7}} \dot{M}_n \dot{\bar{\psi}}_n ds \\ & - \int_{\Gamma_{e9}} \dot{M}_{ns} \dot{\bar{\psi}}_s ds - \int_{\Gamma_{e6}} (\dot{R} - \bar{R}^*) \dot{w} ds \\ & - \int_{\Gamma_{e8}} (\dot{M}_n - \dot{\bar{M}}_n) \dot{\psi}_n ds - \int_{\Gamma_{e10}} (\dot{M}_{ns} - \dot{\bar{M}}_{ns}) \dot{\psi}_s ds \\ & + \frac{1}{2}\int_{\Gamma_e} \mathbf{t}_{\text{out}} \mathbf{u}_{\text{out}} ds - \int_{\Gamma_{e11}} \mathbf{t}_{\text{out}} \tilde{\mathbf{u}}_{\text{out}} ds \end{aligned} \tag{248}$$

where

$$\begin{aligned} \Gamma_e = & \Gamma_{e1} + \Gamma_{e2} + \Gamma_{e11} = \Gamma_{e3} + \Gamma_{e4} + \Gamma_{e11} = \Gamma_{e5} + \Gamma_{e6} + \Gamma_{e11} = \Gamma_{e7} \\ & + \Gamma_{e8} + \Gamma_{e11} = \Gamma_{e9} + \Gamma_{e10} + \Gamma_{e11} \end{aligned} \tag{249}$$

with

$$\begin{aligned} & \Gamma_{e1} = \Gamma_e \cap \Gamma_{u_n}, \quad \Gamma_{e2} = \Gamma_e \cap \Gamma_{N_n}, \quad \Gamma_{e3} = \Gamma_e \cap \Gamma_{u_s} \\ & \Gamma_{e4} = \Gamma_e \cap \Gamma_{N_{ns}}, \quad \Gamma_{e5} = \Gamma_e \cap \Gamma_w, \quad \Gamma_{e6} = \Gamma_e \cap \Gamma_R \\ & \Gamma_{e7} = \Gamma_e \cap \Gamma_{\psi_n}, \quad \Gamma_{e8} = \Gamma_e \cap \Gamma_{M_n}, \quad \Gamma_{e9} = \Gamma_e \cap \Gamma_{\psi_s}, \quad \Gamma_{e10} \\ & = \Gamma_e \cap \Gamma_{M_{ns}} \end{aligned} \tag{250}$$

and Γ_{e11} representing the inter-element boundary of the element.

The extension to thick plates on elastic foundation is similar to that in Sec. 5. In the case of thick plates on an elastic foundation, the formulation presented in this section holds true provided that the following modifications have been made:

a. The interpolation function $\mathbf{N}_{\text{out}}$ should be formed from a suitably truncated complete system of Eqs. (134) and (155) rather than Eqs. (134) and (135).
b. The source function $(w^*, \psi_1^*, \psi_2^*)$, used in calculating the particular solution $\breve{\mathbf{u}}_{\text{out}}$ is now replaced by [22]

$$\begin{aligned} w^*(r_{PQ}) = & AC_2 K_0(r_{PQ}\sqrt{C_2})(1 - DC_2/C) \\ & + BC_1 Y_0(r_{PQ}\sqrt{C_1})(1 + DC_2/C) \end{aligned} \tag{251}$$

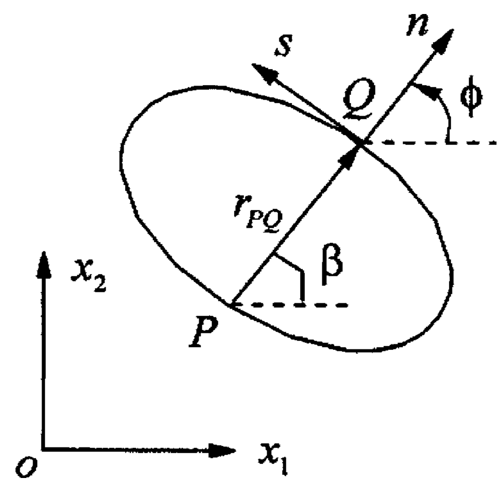

Fig. 9 Illustration for β and ϕ

$$\begin{aligned} \psi_1^*(r_{PQ}) = & -[B\sqrt{C_1} Y_1(r_{PQ}\sqrt{C_1}) \\ & + A\sqrt{C_2} K_1(r_{PQ}\sqrt{C_2})]\cos(\beta - \phi) \end{aligned} \tag{252}$$

$$\begin{aligned} \psi_2^*(r_{PQ}) = & -[B\sqrt{C_1} Y_1(r_{PQ}\sqrt{C_1}) \\ & + A\sqrt{C_2} K_1(r_{PQ}\sqrt{C_2})]\sin(\beta - \phi) \end{aligned} \tag{253}$$

where β and ϕ are defined in Fig. 9, C_1 and C_2 are defined in Eqs. (157) and (158), and

$$A = \frac{1}{2\pi D(C_1 + C_2)}, \quad B = -\frac{1}{4D(C_1 + C_2)} \tag{254}$$

10 Numerical Examples

This section briefly describes some representative numerical examples to illustrate applications of the Trefftz-element approach discussed above.

Example 1: A Skew Crack in a Square Plate Under Uniform Tension. To show the efficiency of the special purpose element, a skew crack in a square plate under tension $\bar{p}$ is considered (Fig. 10). For comparison, the element mesh used is the same as that of Jirousek et al. [59]. Using the formulations (93) and (94), one can easily prove that

$$K_I = \beta_1 \sqrt{2\pi w}, \quad K_{II} = \eta_1 \sqrt{2\pi w} \tag{255}$$

The results for stress intensity factors are listed in Table 2 and comparison is made to those obtained by the conventional

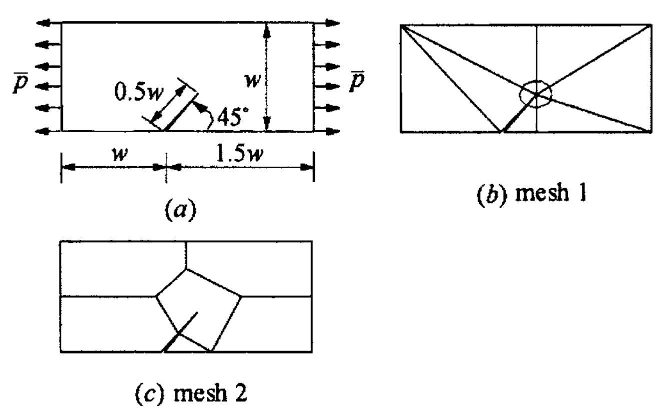

Fig. 10 Stretched skew crack plate (μ=0.3)

Table 2 Comparison of various predictions of K_I and K_{II} for the skew crack problem from Fig. 10. Conventional results (mesh 1) taken from [59] (CIM=contour integral method, CFM=cutoff function method). HT results (mesh 2) obtained from Eq. (255).

	$K_I/\bar{p}\sqrt{2\pi w}$			$K_{II}/\bar{p}\sqrt{2\pi w}$		
	Conv. p elem.[a]			Conv. p elem.[a]		
m	CIM	CFM	HT-p	CIM	CFM	HT-p
0	0.54127	0.42259	0.46535	−0.37480	−0.29005	−0.28433
2	0.49708	0.55588	0.59012	−0.25578	−0.28292	−0.28669
4	0.58909	0.56161	0.59983	−0.28951	−0.27474	−0.29067
6	0.57864	0.59232	0.60142	−0.28319	−0.29022	−0.29092
8	0.60588	0.59825	0.60149	−0.29398	−0.29012	−0.29095
10	0.59672	0.60043	0.60151	−0.28997	−0.29097	−0.29096
12	0.60313	0.60119	—	−0.29196	−0.29091	—
14	0.60032	0.60132	—	−0.29042	−0.29095	—

[a]Data taken from [59].

p-element method [59]. It can be seen from Table 2 that the solution from the HT p-element method may converge to a fixed value relatively quickly compared to the conventional p-element method.

Example 2: Morley's Skew Plate Problem (Fig. 11). The performance of a special-purpose corner element in singularity calculations is exemplified by analyzing the well-known Morley's skew plate problem (Fig. 11). For the skew plate angle of 30 deg, the plate exhibits a very strong singularity at the obtuse corners (the exponent of the leading singularity term Cr^{λ} of the deflection expansion is equal to 1.2). Such a problem is considered difficult and has attracted the attention of research workers [29,148,149]. The difficulty is mainly attributable to the strong singularity at the obtuse corner, which causes most FE models either to converge very slowly to the true solution or not to converge at all. The analytical solution of the problem based on the series expansion with coefficients determined by the least-squares method was presented by Morley [150], whose results are generally used as reference.

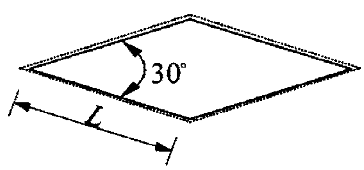

Fig. 11 Uniformly loaded simply supported 30 deg skew plate (L/t=100)

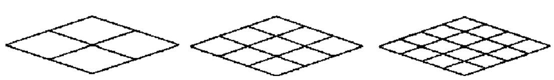

Fig. 12 Configuration of meshes used in finite element analysis

The numerical results for different meshes (2×2, 3×3, 4×4, shown in Fig. 12) are obtained at the plate center and displayed in Tables 3 and 4, and are compared to Morley's results ($w_c=0.000408qL^4/D$, $M_{11c}=0.0108qL^2$ and $M_{22c}=0.0191qL^2$). In the calculation, 10 corner functions have been used.

The high efficiency of special-purpose corner functions for the solution of singularity problems can be seen from Tables 3 and 4. Such functions play an even more important role within the T-element model where, by definition, the expansion basis of each element is optional. This feature enables involved singularity or stress concentration problems to be efficiently solved without troublesome mesh refinement. It is also evident from Tables 3 and 4 that the Trefftz-element model performs well with regard to p convergence, i.e., the numerical results converge quickly to the analytical results along with increase of M.

Example 3: Large Deflection for an Annular Plate on a Pasternak-Type Foundation. The annular plate is subjected to a uniform distributed load q ($Q=qa^4/Et^4$) and rests on a Pasternak-type foundation. The inner boundary of the plate is in a free-edge condition, whereas the outer boundary condition is clamped immovable. Some initial data used in the example are given by

$$G_P a^2/Et^3 = 1, \quad K = k_P a^4/Et^3 = 5, \quad b/a = 1/3, \quad \mu = 1/3$$

where a and b are the outer and inner radii of the annular plate (Fig. 13). In the example, a quarter of the plate is modeled by the three meshes shown in Fig. 13. The loading step is taken as $\Delta Q=5$. Some results obtained by the proposed method are listed in Tables 5 and 6.

11 Conclusions and Future Developments

On the basis of the preceding discussion, the following conclusions can be drawn. In contrast to conventional FE and boundary

Table 3 Solution with special purpose corner functions applied to all corner elements for Morley's simply supported uniformly loaded skew 30 deg plate

		Percentage error			
Mesh quantity		$M=1$	3	5	7
2×2	w_c	−6.08	0.55	0.0	0.0
	M_{11c}	−5.03	3.32	1.08	0.01
	M_{22c}	−27.86	5.44	0.97	0.03
3×3	w_c	−1.98	0.31	0.0	0.0
	M_{11c}	0.92	0.27	0.0	0.0
	M_{22c}	3.25	1.02	0.03	0.0
4×4	w_c	−1.58	0.01	0.0	0.0
	M_{11c}	0.39	0.11	0.0	0.0
	M_{22c}	2.25	0.98	0.01	0.0

Table 4 Solution without special-purpose corner functions for Morley's simply supported uniformly loaded skew plate

Mesh quantity		Percentage error			
		$M=1$	3	5	7
2×2	w_c	−29.45	−6.44	1.46	−1.22
	M_{11c}	−7.45	−7.33	−3.44	−1.55
	M_{22c}	−22.52	−9.89	5.78	3.67
3×3	w_c	−22.98	−4.88	−1.98	0.44
	M_{11c}	−9.55	−6.78	−1.59	−0.76
	M_{22c}	−23.45	−11.55	−2.66	1.65
4×4	w_c	−19.65	−3.98	−1.79	0.34
	M_{11c}	−8.22	−4.95	−1.22	−0.62
	M_{22c}	−19.55	−5.88	3.53	2.12

element models, the main advantages of the HT FE model are: (i) the formulation calls for integration along the element boundaries only, which enables arbitrary polygonal or even curve-sided elements to be generated. As a result, it may be considered as a special, symmetric, substructure-oriented boundary solution approach, which thus possesses the advantages of the boundary element method (BEM). In contrast to conventional boundary element formulation, however, the HT FE model avoids the introduction of singular integral equations and does not require the construction of a fundamental solution, which may be very laborious to build; (ii) the HT FE model is likely to represent the optimal expansion bases for hybrid-type elements where inter-element continuity need not be satisfied, a priori, which is particularly important for generating a quasi-conforming plate bending element; (iii) the model offers the attractive possibility of developing accurate crack singular, corner or perforated elements, simply by using appropriate known local solution functions as the trial functions of the intra-element displacements. Remarkable progress has been achieved in the field of potential flow problems, fracture mechanics, plane elasticity, thin and thick plate bending, elastodynamics, and nonlinear problems of plate bending by the Trefftz FE approach. In addition, Herrera's version of Trefftz method expands very much the scope of the method of Trefftz. In particular, Applications of Trefftz method to non-symmetric problems has been made using Trefftz method.

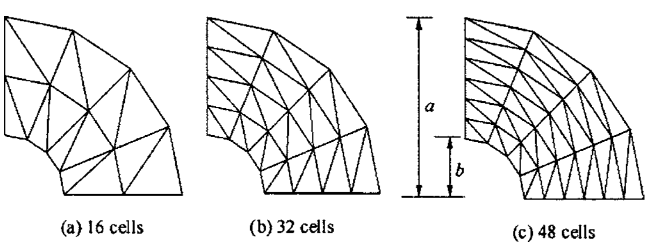

Fig. 13 Three element meshes in Example 3

It is recognized that the Trefftz FE method has become increasingly popular as an efficient numerical tool in computational mechanics since their initiation in the late seventies. However, there are still many possible extensions and areas in need of further development in the future. Among those developments one could list the following:

1. Development of efficient HT FE-BEM schemes for complex engineering structures and the related general purpose computer codes with preprocessing and postprocessing capabilities.
2. Generation of various special-purpose functions to effectively handle singularities attributable to local geometrical or load effects. As discussed previously, the special-purpose functions warrant that excellent results are obtained at minimal computational cost and without local mesh refinement. Extension of such functions could be applied to other cases such as the boundary layer effect between two materials, the interaction between fluid and structure in fluid-structure problems, and circular hole, corner and load singularities.
3. Development of HT FE in conjunction with a topology optimization scheme to contribute to microstructure design.
4. Development of efficient adaptive procedures including error estimation, h-extension element, higher order p-capabilities, and convergence studies.
5. Extensions of HT FE to soil mechanics, thermoelasticity, deep shell structure, fluid flow, piezoelectric materials, and rheology problems.
6. Indirect Trefftz method in conjunction with parallel processing to numerical models of continuous systems of science

Table 5 Maximum deflection w_m/t in Example 3 ($M=0$)

Method	mesh	$Q=10$	15	20	25	30
HT FE	16 cells	0.491	0.725	0.920	1.082	1.227
	32	0.508	0.732	0.929	1.095	1.238
	48	0.513	0.738	0.935	1.105	1.243
Ref. [151]		0.510	0.740	0.930	1.100	1.240

Table 6 Maximum deflection w_m/t versus M in Example 3 (32 cells)

M	0	1	3	5	6	8	10
$Q=10$	0.508	0.512	0.513	0.515	0.518	0.518	0.519
15	0.732	0.735	0.736	0.736	0.739	0.740	0.742
20	0.929	0.933	0.935	0.936	0.940	0.942	0.943
25	1.095	1.099	1.099	1.100	1.103	1.103	1.104
30	1.238	1.242	1.244	1.244	1.248	1.250	1.251

and engineering; Application of the indirect method of Trefftz to space-time problems, including parabolic (heat conduction), hyperbolic (wave propagation) transport (advection-diffusion) equations.

Acknowledgment

The author would like to express his gratitude to S. Adali for his encouragement and to I. Herrera and A. P. Zielinski for providing useful materials. The author also thanks the Australian Research Council for financial support with a professorial fellowship program. Special thanks go to WIT Press who permitted the author to reproduce some contents of his book entitled, *The Trefftz Finite and Boundary Element Method* [61] (for further information see www.witpress.com).

References

[1] Jirousek, J., 1978, "Basis for Development of Large Finite Elements Locally Satisfying All Field Equations," Comput. Methods Appl. Mech. Eng., **14**, pp. 65–92.

[2] Jirousek, J., and Leon, N., 1977, "A Powerful Finite Element for Plate Bending," Comput. Methods Appl. Mech. Eng., **12**, pp. 77–96.

[3] Herrera, I., 1977, "General Variational Principles Applicable to the Hybrid Element Method," Proc. Natl. Acad. Sci. U.S.A., **74**, pp. 2595–2597.

[4] Herrera, I., 1980, "Boundary Methods: A Criterion for Completeness," Proc. Natl. Acad. Sci. U.S.A., **77**, pp. 4395–4398.

[5] Herrera, I., Ewing, R. E., Celia, M. A., and Russell, T., 1993, "Eulerian-Lagrangian Localized Adjoint Method: The Theoretical Framework," Numer. Methods Partial Differ. Equ. **9**, pp. 431–457.

[6] Herrera, I., and Sabina, F. J., 1978, "Connectivity as an Alternative to Boundary Integral Equations: Construction of Bases," Proc. Natl. Acad. Sci. U.S.A., **75**, pp. 2059–2063.

[7] Trefftz, E., 1926, Ein Gegenstück zum Ritzschen Verfahren, *Proc. of 2nd Int. Congress of Applied Mechanics*, Zurich, Robinson and Associates, Bridestowe, pp. 131–137.

[8] Jirousek, J., and N'Diaye, M., 1990, "Solution of Orthotropic Plates Based on *p*-Extension of the Hybrid-Trefftz Finite Element Model," Comput. Struct., **34**, pp. 51–62.

[9] Jirousek, J., and Wroblewski, A., 1996, "T-Elements: State of the Art and Future Trends," Arch. Comput. Methods Eng., **3**, pp. 323–434.

[10] Diab, S. A., 2001, "The Natural Boundary Conditions as a Variational Basis for Finite Element Methods," Comput. Assist. Mech. Eng. Sci., **8**, pp. 213–226.

[11] Freitas, J. A. T., and Ji, Z. Y., 1996, "Hybrid-Trefftz Equilibrium Model for Crack Problems," Int. J. Numer. Methods Eng., **39**, pp. 569–584.

[12] Herrera, I., 2001, "On Jirousek Method and its Generalization," Comput. Assist. Mech. Eng. Sci., **8**, pp. 325–342.

[13] Jirousek, J., and Venkatesh, A., 1989, "A Simple Stress Error Estimator for Hybrid-Trefftz *p*-Version Elements," Int. J. Numer. Methods Eng., **28**, pp. 211–236.

[14] Kita, E., Kamiya, N., and Ikeda, Y., 1996, "New Boundary-Type Scheme for Sensitivity Analysis Using Trefftz Formulation," Finite Elem. Anal. Design **21**, pp. 301–317.

[15] Lifits, S., Reutskiy, S., and Tirozzi, B., 1997, "Trefftz Spectral Method for Initial-Boundary Problems," Comput. Assist. Mech. Eng. Sci., **4**, pp. 549–565.

[16] Markiewicz, M., and Mahrenholtz, O., 1997, "Combined Time-Stepping and Trefftz Approach for Nonlinear Wave-Structure Interaction," Comput. Assist. Mech. Eng. Sci., **4**, pp. 567–586.

[17] Maunder, E. A. W., and Almeida, J. P. M., 1997, "Hybrid-Equilibrium Elements With Control of Spurious Kinematic Modes," Comput. Assist. Mech. Eng. Sci., **4**, pp. 587–605.

[18] Melenk, J. M., and Babuska, I., 1997, "Approximation With Harmonic and Generalized Harmonic Polynomials in the Partition of Unity Method," Comput. Assist. Mech. Eng. Sci. **4**, pp. 607–632.

[19] Ohnimus, S., Rüter, M., and Stein, E., 2001, "General Aspects of Trefftz Method and Relations to Error Estimation of Finite Element Approximations," Comput. Assist. Mech. Eng. Sci., **8**, pp. 425–437.

[20] Peters, K., and Wagner, W., 1994, "New Boundary-Type Finite Element for 2-D and 3-D Elastic Structures," Int. J. Numer. Methods Eng., **37**, pp. 1009–1025.

[21] Piltner, R., 1997, "On the Systematic Construction of Trial Functions for Hybrid Trefftz Shell Elements," Comput. Assist. Mech. Eng. Sci., **4**, pp. 633–644.

[22] Qin, Q. H., 1994, "Hybrid Trefftz Finite Element Approach for Plate Bending on an Elastic Foundation," Appl. Math. Model., **18**, pp. 334–339.

[23] Zheng, X. P., and Yao, Z. H., 1995, "Some Applications of the Trefftz Method in Linear Elliptic Boundary-Value Problems," Adv. Eng. Software, **24**, pp. 133–145.

[24] Jirousek, J., and Teodorescu, P., 1982, "Large Finite Elements Method for the Solution of Problems in the Theory of Elasticity," Comput. Struct., **15**, pp. 575–587.

[25] Jirousek, J., and Venkatesh, A., 1992, "Hybrid-Trefftz Plane Elasticity Elements With *p*-Method Capabilities," Int. J. Numer. Methods Eng., **35**, pp. 1443–1472.

[26] Leitao, V. M. A., 2001, "Comparison of Galerkin and Collocation Trefftz Formulations for Plane Elasticity," Comput. Assist. Mech. Eng. Sci., **8**, pp. 397–407.

[27] Piltner, R., 1985, "Special Finite Elements With Holes and Internal Cracks," Int. J. Numer. Methods Eng., **21**, pp. 1471–1485.

[28] Stein, E., and Peters, K., 1991, "A New Boundary-Type Finite Element for 2D and 3D Elastic Solids," *The Finite Element Method in the 1990s, A Book Dedicated to OC Zienkiewicz*, E. Onate, J. Periaux, and A. Samuelson eds., Springer, Berlin, pp. 35–48.

[29] Jirousek, J., 1987, "Hybrid-Trefftz Plate Bending Elements With *p*-Method Capabilities," Int. J. Numer. Methods Eng., **24**, pp. 1367–1393.

[30] Jirousek, J., and Guex, L., 1986, "The Hybrid-Trefftz Finite Element Model and Its Application to Plate Bending," Int. J. Numer. Methods Eng., **23**, pp. 651–693.

[31] Jirousek, J., Szybinski, B. and Zielinski, A. P., 1997, "Study of a Family of Hybrid-Trefftz Folded Plate *p*-Version Elements," Comput. Assist. Mech. Eng. Sci., **4**, pp. 453–476.

[32] Jin, F. S., and Qin, Q. H., 1995, "A Variational Principle and Hybrid Trefftz Finite Element for the Analysis of Reissner Plates, Comput. Struct., **56**, pp. 697–701.

[33] Jirousek, J., Wroblewski, A., Qin, Q. H., and He, X. Q., 1995, "A Family of Quadrilateral Hybrid Trefftz *p*-Element for Thick Plate Analysis," Comput. Methods Appl. Mech. Eng., **127**, pp. 315–344.

[34] Jirousek, J., Wroblewski, A., and Szybinski, B., 1995, "A New 12 DOF Quadrilateral Element for Analysis of Thick and Thin Plates," Int. J. Numer. Methods Eng., **38**, pp. 2619–2638.

[35] Maunder, E. A. W., 2001, "A Trefftz Patch Recovery Method for Smooth Stress Resultants and Applications to Reissner-Mindlin Equilibrium Plate Models," Comput. Assist. Mech. Eng. Sci., **8**, pp. 409–424.

[36] Qin, Q. H., 1995, "Hybrid Trefftz Finite Element Method for Reissner Plates on an Elastic Foundation," Comput. Methods Appl. Mech. Eng., **122**, pp. 379–392.

[37] Petrolito, J., 1990, "Hybrid-Trefftz Quadrilateral Elements for Thick Plate Analysis," Comput. Methods Appl. Mech. Eng., **78**, pp. 331–351.

[38] Petrolito, J., 1996, "Triangular Thick Plate Elements Based on a Hybrid-Trefftz Approach," Comput. Struct., **60**, pp. 883–894.

[39] Piltner, R., 1992, A Quadrilateral Hybrid-Trefftz Plate Bending Element for the Inclusion of Warping Based on a Three-Dimensional Plate Formulation," Int. J. Numer. Methods Eng., **33**, pp. 387–408.

[40] Piltner, R., 1989, "On the Representation of Three-Dimensional Elasticity Solutions With the Aid of Complex Value Functions," J. Elast., **22**, pp. 45–55.

[41] Wroblewski, A., Zielinski, A. P., and Jirousek, J., 1992, "Hybrid-Trefftz *p*-Element for 3-D Axisymmetric Problems of Elasticity", *Numerical Methods in Engineering '92, Proc. First Europ. Conf. on Numer. Meth. in Eng.*, C. Hirsch, O. C. Zienkiewicz, and E. Onãte, eds., Elsevier, Brussels, pp. 803–810.

[42] Jirousek, J., and Stojek, M., 1995, "Numerical Assessment of a New T-Element Approach," Comput. Struct., **57**, pp. 367–378.

[43] Zielinski, A. P., and Zienkiewicz, O. C., 1985, "Generalized Finite Element Analysis With T-Complete Boundary Solution Functions," Int. J. Numer. Methods Eng., **21**, pp. 509–528.

[44] Vörös, G. M., and Jirousek, J., 1991, "Application of the Hybrid-Trefftz Finite Element Model to Thin Shell Analysis," *Proc. Europ. Conf. on New Advances in Comp. Struc. Mech.*, P. Ladeveze and O. C. Zienkiewicz, eds., Elsevier, Giens, France, pp. 547–554.

[45] Freitas, J. A. T., 1997, "Hybrid-Trefftz Displacement and Stress Elements for Elasto-Dynamic Analysis in the Frequency Domain," Comput. Assist. Mech. Eng. Sci., **4**, pp. 345–368.

[46] Jirousek, J., 1997, "A T-Element Approach to Forced Vibration Analysis and Its Application to Thin Plates," LSC Internal Report 97/03, Swiss Federal Institute of Technology, Lausanne.

[47] Qin, Q. H., 1996, "Transient Plate Bending Analysis by Hybrid Trefftz Element Approach," Commun. Numer. Methods Eng., **12**, pp. 609–616.

[48] Jirousek, J., and Qin, Q. H. 1996, "Application of Hybrid-Trefftz Element Approach to Transient Heat Conduction Analysis," Comput. Struct., **58**, pp. 195–201.

[49] Qin, Q. H., 1995, "Postbuckling Analysis of Thin Plates by a Hybrid Trefftz Finite Element Method," Comput. Methods Appl. Mech. Eng., **128**, pp. 123–136.

[50] Qin, Q. H., 1996, "Nonlinear Analysis of Thick Plates by HT FE Approach," Comput. Struct., **61**, pp. 271–281.

[51] Qin, Q. H., 1997, "Postbuckling Analysis of Thin Plates on an Elastic Foundation by HT FE Approach," Appl. Math. Model., **21**, pp. 547–556.

[52] Qin, Q. H., and Diao, S., 1996, "Nonlinear Analysis of Thick Plates on an Elastic Foundation by HT FE With *p*-Extension Capabilities," Int. J. Solids Struct., **33**, pp. 4583–4604.

[53] Bussamra, F. L. S., Pimenta, P. M., and Freitas, J. A. T., 2001, "Hybrid-Trefftz Stress Elements for Three-Dimensional Elastoplasticity," Comput. Assist. Mech. Eng. Sci., **8**, pp. 235–246.

[54] Freitas, J. A. T., and Wang, Z. M., 1998, "Hybrid-Trefftz Stress Elements for Elastoplasticity," Int. J. Numer. Methods Eng., **43**, pp. 655–683.

[55] Zielinski, A. P., 1988, "Trefftz Method: Elastic and Elastoplastic Problems," Comput. Methods Appl. Mech. Eng., **69**, pp. 185–204.

[56] Qin, Q. H., 2003, "Variational Formulations for TFEM of Piezoelectricity," Int. J. Solids Struct., **40**, pp. 6335–6346.

[57] Qin, Q. H., 2003, "Solving Anti-Plane Problems of Piezoelectric Materials by the Trefftz Finite Element Approach," Comput. Mech., **31**, pp. 461–468.
[58] Venkatesh, A., and Jirousek, J., 1995, "Accurate Representation of Local Effect Due to Concentrated and Discontinuous Loads in Hybrid-Trefftz Plate Bending Elements," Comput. Struct., **57**, pp. 863–870.
[59] Jirousek, J., Venkatesh, A., Zielinski, A. P., and Rabemanantsoo, H., 1993, "Comparative Study of *p*-Extensions Based on Conventional Assumed Displacement and Hybrid-Trefftz FE Models," Comput. Struct., **46**, pp. 261–278.
[60] Huang, H. T., and Li, Z. C., 2003, "Global Superconvergence of Adini's Elements Coupled With Trefftz Method for Singular Problems," Eng. Anal. Boundary Elem., **27**, pp. 227–240.
[61] Qin, Q. H., 2000, *The Trefftz Finite and Boundary Element Method*, WIT Press, Southampton.
[62] Herrera, I., 1997, "Trefftz-Herrera Method," Comput. Assist. Mech. Eng. Sci., **4**, pp. 369–382.
[63] Jirousek, J., 1991, "New Trends in HT-*p* Element Approach," *The Finite Element Method in the 1990s*, E. Onate, J. Periaux, and A. Samuelson, eds., Springer, Berlin.
[64] Jirousek, J., and Wroblewski, A., 1995, "T-Elements: A Finite Element Approach With Advantages of Boundary Solution Methods, Adv. Eng. Software **24**, 71-88.
[65] Jirousek, J., and Zieliński, A. P., 1997, "Survey of Trefftz-Type Element Formulations," Comput. Struct., **63**, pp. 225–242.
[66] Kita, E., and Kamiya, N., 1995, "Trefftz Method: An Overview," Adv. Eng. Software, **24**, pp. 3–12.
[67] Qin, Q. H., 1993, "A Brief Introduction and Prospect to Hybrid-Trefftz Finite Elements," Mech. Pract., **15**, pp. 20–22 (in Chinese).
[68] Qin, Q. H., 1998, "The Study and Prospect of Hybrid-Trefftz Finite Element Method," Adv. Mech., **28**, pp. 71–80 (in Chinese).
[69] Zienkiewicz, O. C., 1997, "Trefftz Type Approximation and the Generalised Finite Element Method: History and Development," Comput. Assist. Mech. Eng. Sci., **4**, pp. 305–316.
[70] Gourgeon, H., and Herrera, I., 1981, "Boundary Methods: C-Complete Systems for Biharmonic Equations," *Boundary Element Methods*, C. A. Brebbia, ed., pp. 431–441, Springer-Verlag, Berlin.
[71] Herrera, I., 1977, "Theory of Connectivity Formal Symmetric Operators," Proc. Natl. Acad. Sci. U.S.A., **74**, pp. 4722–4725.
[72] Celia, M., and Herrera, I., 1987, "Solution of General Differential Equations Using the Algebraic Theory Approach," Numer. Methods Partial Differ. Equ., **3**, pp. 117–129.
[73] Herrera, I., 1987, "The Algebraic Theory Approach for Ordinary Differential Equations: Highly Accurate Finite Differences," Numer. Methods Partial Differ. Equ., **3**, pp. 199–218.
[74] Herrera, I., 1992, "Localized Adjoint Methods: A New Discretization Methodology," *Computational Methods in Geosciences*, W. E. Fitzgibbon and M. F. Wheeler, eds., SIAM, Philadelphia, Chap. 6, pp. 66–77.
[75] Herrera, I., 2000, "Trefftz Method: A General Theory," Numer. Methods Partial Differ. Equ., **16**, pp. 561–580.
[76] Herrera, I., 2002, "The Indirect Approach to Domain Decomposition," *14th Int. Conf. on Domain Decomposition Methods*, Cocoyoc, Mor., Mex., Invited Plenary Lecture, www.ddm.org
[77] Herrera, I. 2002, "A Unified Theory of Domain Decomposition Methods," *14th Int. Conf. on Domain Decomposition Methods*, Cocoyoc, Mor., Mex., www.ddm.org
[78] Herrera, I., and Yates, R., 2001, "General Theory of Domain Decomposition: Beyond Schwarz Methods," Numer. Methods Partial Differ. Equ., **17**, pp. 495–517.
[79] Herrera, I., Yates, R., and Diaz, M., 2002, "General Theory of Domain Decomposition: Indirect Methods," Numer. Methods Partial Differ. Equ., **18**, pp. 296–322.
[80] Díaz, M., Herrera, I., and Yates, R., 2002, "Indirect Method of Collocation," *14th Int. Conf. on Domain Decomposition Methods*, Cocoyoc, Mor., Mex., www.ddm.org
[81] Yates, R., and Herrera, I., 2002, "Parallel Implementation of Indirect Collocation Methods," *14th Int. Conf. on Domain Decomposition Methods*, Cocoyoc, Mor., Mex. www.ddm.org
[82] Herrera, I., 1985, "Unified Approach to Numerical Methods. I. Green's Formulas for Operators in Discontinuous Fields," Numer. Methods Partial Differ. Equ., **1**, pp. 12–37.
[83] Herrera, I., Chargoy, L., and Alduncin, G., 1985, "Unified Approach to Numerical Methods. Part 3. Finite Differences and Ordinary Differential Equations," Numer. Methods Partial Differ. Equ., **1**, pp. 241–258.
[84] Jirousek, J., 1993, "Variational Formulation of Two Complementary Hybrid-Trefftz FE Models," Commun. Numer. Methods Eng., **9**, pp. 837–845.
[85] Jirousek, J., and Zielinski, A. P., 1993, "Dual Hybrid-Trefftz Element Formulation Based on Independent Boundary Traction Frame," Int. J. Numer. Methods Eng., **36**, pp. 2955–2980.
[86] Cheung, Y. K., Jin, W. G., and Zienkiewicz, O. C., 1989, "Direct Solution Procedure for Solution of Harmonic Problems Using Complete, Non-Singular, Trefftz Functions," Commun. Appl. Numer. Methods, **5**, pp. 159–169.
[87] Cheung, Y. K., Jin, W. G., and Zienkiewicz, O. C., 1991, "Solution of Helmholtz Equation by Trefftz Method," Int. J. Numer. Methods Eng., **32**, pp. 63–78.
[88] Jirousek, J., and Wroblewski, A., 1994, "Least-Squares T-Elements: Equivalent FE and BE Forms of a Substructure-Oriented Boundary Solution Approach," Commun. Numer. Methods Eng., **10**, pp. 21–32.
[89] Stojek, M., 1998, "Least-Squares Trefftz-Type Elements for the Helmholtz Equation," Int. J. Numer. Methods Eng., **41**, pp. 831–849.
[90] Cialkowski, M. J., 2001, "Trefftz Functions as Basic Functions of FEM in Application to Solution of Inverse Heat Conduction Problem," Comput. Assist. Mech. Eng. Sci., **8**, pp. 247–260.
[91] Desmet, W., Sas, P., and Vandepitte, D., 2001, "An Indirect Trefftz Method for the Steady-State Dynamic Analysis of Coupled Vibro-Acoustic Systems," Comput. Assist. Mech. Eng. Sci., **8**, pp. 271–288.
[92] Hsiao, G. C., Schnack, E., and Wendland, W. L., 2000, "Hybrid Coupled Finite-Boundary Element Methods for Elliptic Systems of Second Order," Comput. Methods Appl. Mech. Eng., **190**, pp. 431–485.
[93] Ihlenburg, F., and Babuska, I., 1997, "Solution of Helmholtz Problems by Knowledge-Based FEM," Comput. Assist. Mech. Eng. Sci., **4**, pp. 397–415.
[94] Kita, E., Kamiya, N., and Ikeda, Y., 1997, "First- and Second-Order Sensitivity Analysis Schemes by Collocation-Type Trefftz Method," Comput. Assist. Mech. Eng. Sci., **4**, pp. 477–489.
[95] Kolodziej, J. A., and Mendes, A. C., 2001, "T-Functions for 2-D Creeping Flow on Domains With Circular Cylinders, Corners, and Processing Symmetry," Comput. Assist. Mech. Eng. Sci., **8**, pp. 359–384.
[96] Kolodziej, J. A., and Uscilowska, A., 1997, "Trefftz-Type Procedure for Laplace Equation on Domains With Circular Holes, Circular Inclusions, Corners, Slits, and Symmetry," Comput. Assist. Mech. Eng. Sci. **4**, pp. 501–519.
[97] Stojek, M., Markiewicz, M., and Mahrenholtz, O., 2000, "Diffraction Loads on Multiple Vertical Cylinders With Rectangular Cross Section by Trefftz-Type Finite Elements," Comput. Struct., **75**, pp. 335–345.
[98] Zielinski, A. P., 1997, "Special Trefftz Elements and Improvement of Their Conditioning," Commun. Numer. Methods Eng., **13**, pp. 765–775.
[99] Freitas, J. A. T., and Bussamra, F. L. S., 2000, "Three-Dimensional Hybrid-Trefftz Stress Elements," Int. J. Numer. Methods Eng., **47**, pp. 927–950.
[100] Freitas, J. A. T., and Cismasiu, I., 2002, "Shape Optimizing With Hybrid-Trefftz Displacement Elements," Int. J. Numer. Methods Eng., **53**, pp. 473–498.
[101] Hsiao, G. C., Schnack, E., and Wendland, W. L., 1999, "A Hybrid Coupled Finite-Boundary Element Method in Elasticity," Comput. Methods Appl. Mech. Eng., **173**, pp. 287–316.
[102] Jin, W. G., Cheung, Y. K., and Zienkiewicz, O. C., 1990, "Application of Trefftz Method in Plane Elasticity," Int. J. Numer. Methods Eng., **30**, pp. 1147–1161.
[103] Qin, Q. H., 2004, "Dual Variational Formulation for Trefftz Finite Element Method of Elastic Materials," Mech. Res. Commun., **31**, pp. 321–330.
[104] Kompis, V., Konkol, F., and Vasko, M., 2001, "Trefftz-Polynomial Reciprocity Based FE Formulations," Comput. Assist. Mech. Eng. Sci., **8**, pp. 385–395.
[105] Kompis, V., Pavol, N., and Mariam, H., 2002, "Finite Displacements in Reciprocity-Based FE Formulation," Comput. Assist. Mech. Eng. Sci., **9**, pp. 469–480.
[106] Sladek, J., and Sladek, V., 2002, "A Trefftz Function Approximation in Local Boundary Integral Equations," Comput. Mech., **28**, pp. 212–219.
[107] Sladek, J., Sladek, V., Kompis, V., and Van Keer, R., 2000, "Application of Multi-Region Trefftz Method to Elasticity," Comput. Model. Eng. Sci., **1**, pp. 1–8.
[108] Jin, W. G., Cheung, Y. K., and Zienkiewicz, O. C., 1993, "Trefftz Method for Kirchhoff Plate Bending Problems," Int. J. Numer. Methods Eng., **36**, pp. 765–781.
[109] Jirousek, J., Zieliński, A. P., and Wróblewski, A. 2001, "T-Element Analysis of Plates on Unilateral Elastic Winkler-Type Foundation," Computer Assisted Mech. Eng. Sci., **8**, pp. 343–358.
[110] Venkatesh, A. and Jirousek, J., 1987, "An Improved 9 DOF Hybrid-Trefftz Triangular Element for Plate Bending," Eng. Comput., **4**, pp. 207–222.
[111] Brink, U., Kkreienmeyer, M., Peters, K., and Stein, E., 1997, "Aspects of Trefftz Method in BEM and FEM and Their Coupling," Comput. Assist. Mech. Eng. Sci., **4**, pp. 327–344.
[112] Chang, J. R., Liu, R. F., Yeih, W. C., and Kuo, S. R., 2002, "Applications of the Direct Trefftz Boundary Element Method to the Free-Vibration Problem of a Membrane," J. Acoust. Soc. Am., **112**, pp. 518–527.
[113] Freitas, J. A. T., 2002, "Mixed Finite Element Formulation for the Solution of Parabolic Problems," Comput. Methods Appl. Mech. Eng., **191**, pp. 3425–3457.
[114] Gyimesi, M., Wang, J. S., and Ostergaard, D., 2001, "Hybrid *p*-Element and Trefftz Method for Capacitance Computation," IEEE Trans. Magn., **37**, pp. 3680–3683.
[115] He, J. H., 2002, "Generalized Variational Principles for Thermopiezoelectricity," Arch. Appl. Mech., **72**, pp. 248–256.
[116] Jirousek, J., and Venkatesh, A., 1990, "A New FE Approach for Adaptive Reliability Assurance," Comput. Struct., **37**, pp. 217–230.
[117] Karaś, M., and Zielinski, A. P., 2000, "Parametric Structural Shape Optimization Using the Global Trefftz Approach," Theor Appl. Mech., **38**, pp. 285–296.
[118] Kompis, V., and Jakubovicova, L., 2000, "Errors in Modeling High Order Gradient Fields Using Reciprocity Based FEM," Int. J. Eng. Model., **13**, pp. 27–34.
[119] Olegovich, Y., 2002, "Trefftz Finite Elements for Electromagnetics," IEEE Trans. Microwave Theory Tech., **50**, pp. 1328–1339.
[120] Onuki, T., Wakao, S., Kuwahara, T., and Im, J. W., 1997, "Hybrid Trefftz and Finite Element Method Applied to Magnetic Field Analysis for Rotating Machines," IEEE Trans. Magn., **33**, pp. 2014–2017.
[121] Reutskiy, S., 2002, "A Boundary Method of Trefftz Type With Approximate Trial Functions," Eng. Anal. Boundary Elem., **26**, pp. 341–353.

[122] Szybiński, B., Wróblewski, A., Zieliński, A. P., 2001, "General Strategy of *h-p* Adaptive Solutions in Structural Trefftz-Type Element Analysis," Comput. Assist. Mech. Eng. Sci., **8**, pp. 469–477.
[123] Zieliński, A. P., and Herrera, I., 1987, "Trefftz Method: Fitting Boundary Conditions," Int. J. Numer. Methods Eng., **24**, pp. 871–891.
[124] Zieliński, A. P., Sanecki, H., and Karaś, M., 2001, "Effectiveness of the Trefftz Method in Different Engineering Optimization Procedures," Comput. Assist. Mech. Eng. Sci., **8**, pp. 479–493.
[125] Colton, D. L., 1976, *Partial Differential Equations in the Complex Domain*, Pitman, London.
[126] Henrici, P., 1960, "Complete Systems of Solutions for a Class of Singular Elliptic Partial Differential Equations, *Boundary problems in differential equations*, R. E. Langer, ed., University of Wisconsin Press, Madison.
[127] Herrera, I., 1984, *Boundary Method: An Algebraic Theory*, Pitman, Boston.
[128] Sánchez, S. F. J., Herrera, I., and Avilés, J., 1982, A Boundary Method for Elastic Wave Diffraction. Application to Scattering of SH-Waves by Surface Irregularities, Bull. Seismol. Soc. Am. **72**, 473-490.
[129] Fung, Y. C., 1965, *Foundations of Solid Mechanics*, Prentice-Hall, Englewood Cliffs, NJ.
[130] Love, A. E. H., 1944, *A Treatise on the Mathematical Theory of Elasticity*, Dover, New York.
[131] Malvern, L. E., 1969, *Introduction to the Mechanics of a Continuous Medium*, Prentice-Hall, Englewood Cliffs, NJ.
[132] Muskhelishvili, N. I., 1953, *Some Basic Problems of the Mathematical Theory of Elasticity*, Noordhoff, Groningen, Holland.
[133] Sternberg, E., 1960, "On Some Recent Developments in the Linear Theory of Elasticity," *Proc. 1st Symp. on Naval Structural Mechanics*, J. N. Goodier and N. J. Hoff, eds., Pergamon Press, New York.
[134] Williams, M. L., 1952, "Stress Singularities Resulting From Various Boundary Conditions in Angular Corners of Plates in Extension," J. Appl. Mech., **19**, pp. 526–528.
[135] Lin, K. Y., and Tong, P., 1980, "Singular Finite Elements for the Fracture Analysis of V-Notched Plate," Int. J. Numer. Methods Eng., **15**, pp. 1343–1354.
[136] Xu, Z., 1992, "A Thick-Thin Triangular Plate Element," Int. J. Numer. Methods Eng., **33**, pp. 963–973.
[137] Aminpour, M. A., 1992, "Direct Formulation of a Hybrid 4-Node Shell Element With Drilling Degrees of Freedom," Int. J. Numer. Methods Eng., **35**, pp. 997–1013.
[138] Ibrahimbergovic, A., 1993, "Quadrilateral Finite Elements for Analysis of Thick and Thin Plates," Comput. Methods Appl. Mech. Eng., **110**, pp. 195–209.
[139] Taylor, R. L., and Auricchio, F. A., 1993, "Linked Interpolation for Reissner-Mindlin Plate Elements. Part II. A Simple Triangle," Int. J. Numer. Methods Eng., **36**, pp. 3057–3066.
[140] Zienkiewicz, O. C., Xu, Z., Zeng, L. F., Samuelson, A., and Wiberg, N. E., 1993, "Linked Interpolation for Reissner-Mindlin Plate Elements. Part I. A Simple Quadrilateral," Int. J. Numer. Methods Eng., **36**, pp. 3043–3056.
[141] Mindlin, R. D., 1951, "Influence of Rotatory Inertia and Shear on Flexural Motion of Isotropic Elastic Plates," J. Appl. Mech., **18**, pp. 31–38.
[142] Reissner, E., 1945, "The Effect of Shear Deformation on the Bending of Elastic Plates," J. Appl. Mech., **12**, pp. 69–76.
[143] Hu, H. C., 1963, "On Some Problems of the Antisymmetrical Small Deflection of Isotropic Sandwich Plate," Acta Mech. Sin. **6**, pp. 53–60 (in Chinese).
[144] Reismann, H., 1988, *Elastic Plates: Theory and Applications*, Wiley, New York.
[145] Qin, Q. H., 1998, "Nonlinear Analysis of Plate Bending by Boundary Element Method," *Plate Bending Analysis With Boundary Elements*, M. H. Aliabadi, ed., Computational Mechanics Publications, Southampton, Chap. 8.
[146] Qin, Q. H., and Huang, Y. Y., 1990, "BEM of Postbuckling Analysis of Thin Plates," Appl. Math. Model., **14**, pp. 544–548.
[147] Qin, Q. H., 1993, "Nonlinear Analysis of Reissner Plates on an Elastic Foundation by the BEM," Int. J. Solids Struct., **30**, pp. 3101–3111.
[148] Argyris, J. H., and Lochner, N., 1972, "On the Application of SHEBA Shell Element," Comput. Methods Appl. Mech. Eng., **1**, pp. 317–347.
[149] Wang, D. W., Katz, I. N., and Szabo, B. A., 1984, "*h*- and *p*-Version Finite Element Analysis of Rhombic Plate," Int. J. Numer. Methods Eng., **20**, pp. 1399–1405.
[150] Morley, L. S. D., 1963, *Skew Plates and Structures*, Pergamon Press, London.
[151] Smaill, J. S., 1991, "Large Deflection Response of Annular Plates on Pasternak Foundations," Int. J. Solids Struct., **27**, pp. 1073–1084.

Qing-Hua Qin *received his Bachelor of Engineering degree in Mechanical Engineering from Xi'an Highway University (currently Chang An University), China in 1982, earning his Master of Science degree in 1984 and Doctoral degree in 1990 from Huazhong University of Science and Technology (HUST) in China. Both degrees are in Applied Mechanics. He joined the Department of Mechanics as an Associate Lecturer at HUST in 1984, where he was until 1995. After spending ten years lecturing at HUST, he was awarded the DAAD/K.C. Wong research fellowship in 1994, which enabled him to work at the University of Stuttgart in Germany for nine months. In 1995 he left HUST to take up a postdoctoral fellowship at Tsinghua University, China. He was awarded a Queen Elizabeth II fellowship in 1997 and a professorial fellowship in 2002, both by the Australian Research Council, and is currently working in the Department of Engineering at the Australian National University, Australia. He has authored more than 100 published scientific papers and two books in the field of applied mechanics, and was a recipient of the J.G. Russell Award from the Australian Academy of Science.*